

~~CONFIDENTIAL~~

NACA RM A58F03



RESEARCH MEMORANDUM

WIND-TUNNEL INVESTIGATION OF THE LOW-SPEED AERODYNAMIC
CHARACTERISTICS OF A HYPERSONIC GLIDER CONFIGURATION

By Mark W. Kelly

Ames Aeronautical Laboratory
Moffett Field, Calif.

LIBRARY COPY

CLASSIFICATION CHANGED

SEP 15 1958

UNCLASSIFIED

LANGLEY AERONAUTICAL LABORATORY
LIBRARY, NACA
LANGLEY FIELD, VIRGINIA

To _____

By authority of TPA #39 Date 1/12/66
709-jur

CLASSIFIED DOCUMENT

This material contains information affecting the National Defense of the United States within the meaning of the espionage laws, Title 18, U.S.C., Secs. 793 and 794, the transmission or revelation of which in any manner to unauthorized person is prohibited by law.

NATIONAL ADVISORY COMMITTEE FOR AERONAUTICS

WASHINGTON

September 15, 1958

~~CONFIDENTIAL~~

UNCLASSIFIED

UNCLASSIFIED

NACA RM A58F03

NATIONAL ADVISORY COMMITTEE FOR AERONAUTICS

RESEARCH MEMORANDUM

WIND-TUNNEL INVESTIGATION OF THE LOW-SPEED AERODYNAMIC
CHARACTERISTICS OF A HYPERSONIC GLIDER CONFIGURATION*

By Mark W. Kelly

SUMMARY

A wind-tunnel investigation was made of the low-speed aerodynamic characteristics of an airplane configuration designed to obtain high lift-drag ratios at hypersonic speeds. Six-component force data were obtained for a range of Reynolds numbers from 5.35×10^6 to 10.7×10^6 . Calculations were made of the power-off landing flare of a hypothetical airplane having this configuration, and the results are compared with landing flares obtained in flight of an airplane having lift-drag ratios of the same order of magnitude.

The results of the investigation indicate that the power-off landing of such an aircraft would be a difficult task, primarily because of the high sinking speeds inherent in such a design. If power were provided for use in the landing approach to reduce these sinking speeds to normal values, landings could be accomplished in a more conventional manner.

INTRODUCTION

An airplane configuration designed to obtain high lift-drag ratios at hypersonic speeds by utilizing favorable interference of the fuselage pressure field on the wing is proposed in references 1 and 2. The configuration employs a low-aspect-ratio arrowhead plan-form wing mounted on top of the fuselage. The wing tips are bent down to provide directional stability and to decrease the effective dihedral.

Since it was relatively difficult to estimate the low-speed aerodynamic characteristics of such a configuration, a wind-tunnel investigation to determine these characteristics was undertaken. The main purpose of the investigation was to determine whether or not the low-speed stability and control characteristics of such an airplane would be adequate for landings.

*Title, Unclassified

UNCLASSIFIED

The investigation covered a range of Reynolds numbers (based on fuselage length) from 5.4 million to 10.7 million, corresponding to a dynamic pressure range from 25 to 100 pounds per square foot. Six-component force data were obtained over an angle-of-attack range from 0° to 32° and an angle-of-sideslip range from 0° to 10° . In addition, the effects of changes in the amount of wing-tip droop and changes in wing plan form, and the effectiveness of flap-type controls were determined.

The data obtained from this investigation were used to compute the landing flare path of an aircraft of this type, and a comparison was made with actual flare paths obtained from flight tests of the X-4 airplane.

NOTATION

AR	aspect ratio, $\frac{b^2}{S}$
b	wing span with $\delta_t = 0$, ft
C_D	drag coefficient, $\frac{\text{drag}}{qS}$
C_L	lift coefficient, $\frac{\text{lift}}{qS}$
C_l	rolling-moment coefficient, $\frac{\text{rolling moment}}{qSb}$
$C_{l\beta}$	rate of change of rolling-moment coefficient with sideslip angle
C_m	pitching-moment coefficient, $\frac{\text{pitching moment}}{qSl}$
C_n	yawing-moment coefficient, $\frac{\text{yawing moment}}{qSb}$
$C_{n\beta}$	rate of change of yawing-moment coefficient with sideslip angle
C_Y	side-force coefficient, $\frac{\text{side force}}{qS}$
h	altitude, ft
l	fuselage length, ft
q	free-stream dynamic pressure, lb/sq ft

R	Reynolds number, $\frac{U\ell}{\nu}$
S	wing area, sq ft
t	wing maximum thickness, ft
U	free-stream velocity, fps
V_s	sinking speed, fps
α	angle of attack, deg
β	angle of sideslip, deg
γ	flight path angle, deg
δ_f	flap deflection, deg
δ_{fL}	deflection of left flap, positive to increase lift, deg
δ_{fR}	deflection of right flap, positive to increase lift, deg
δ_r	rudder deflection, deg
δ_t	wing-tip droop, deg (see fig. 1(a))
θ	airplane attitude referred to horizontal, deg
Λ_{LE}	sweepback of wing leading edge, deg
ν	kinematic coefficient of viscosity, sq ft/sec

Subscript

u uncorrected for wind-tunnel wall effects

MODEL AND APPARATUS

The geometric characteristics of the models are shown in figure 1. The wing of plan form A was constructed of Fiberglas molded to an aluminum spar. The wing of plan form C was obtained by bolting 1/32-inch aluminum alloy sheet to the surface of the original wing. (The terminology "plan form A" and "plan form C" corresponds to that used in ref. 1 for these

same configurations.) The vertical fins and wing-body fillets were also cut from sheet metal. Both the single-cone fuselage (figs. 1(a), (b), and (c)) and the 3/4-power fuselage (fig. 1(d)) were made of wood. The delta wing shown in figure 1(c) was made of 1/4-inch plate with the leading edges beveled to a sharp edge at about a 30° angle.

A photograph of plan form A mounted in the Ames 7- by 10-foot wind tunnel is shown in figure 2. The forces and moments were measured with a conventional mechanical balance. The moments for plan forms A and C were referenced to a point at 73 percent of the body length. (The data of ref. 1 indicate that with this center-of-gravity position, plan form A has a static margin of about 7 percent at $M = 5$ and plan form C has a static margin of about 13 percent at $M = 5$.) The moments for the delta wing were referenced to a point at 56.6 percent of the body length to give the same stability at low lift coefficients as that obtained with plan form C to facilitate comparison.

CORRECTIONS

The data were corrected for the effects of wind-tunnel wall interference by the following equations

$$\alpha = \alpha_u + 0.88 C_{L_u}$$

$$C_D = C_{D_u} + 0.015 C_{L_u}^2$$

No corrections for the effects of support interference were made.

RESULTS AND DISCUSSION

Longitudinal Characteristics

Effects of Reynolds number.- Lift, drag, and pitching-moment data for plan form A tested at various Reynolds numbers are presented in figure 3(a). No significant Reynolds number effects are indicated.

Effects of wing-tip droop.- It was proposed that wing-tip droop be used to provide directional stability, and it was shown in reference 1 that relatively large amounts of wing-tip droop gave only small reductions in lift-drag ratio at high supersonic Mach numbers. (For example, the use of 30° of wing-tip droop on plan form A reduced the maximum lift-drag ratio only about 5 percent at $M = 5$.) The main purpose of varying the wing-tip droop in this investigation was to determine the effect of wing-tip droop on the lateral and directional stability and control characteristics and, in particular, to determine whether such a configuration

could be flown as a two-control airplane without the addition of some type of vertical fin. This is discussed more completely in the section entitled "Lateral Characteristics." The following discussion is limited to the effects of wing-tip droop on longitudinal characteristics only. Figure 4(a) shows the effects of varying the amount of wing-tip droop on the longitudinal characteristics of plan form A. Figure 4(b) presents similar data for plan form C. For both plan forms the trends are similar, although the effects for plan form C are more pronounced since more wing area is contained in the drooped tips.

Effect of configuration on static stability.- The pitching-moment curves on both figures 4(a) and (b) indicate a reduction in stability with increasing lift. This was believed to be due to a reduction of lift near the wing tips as the angle of attack was increased, and to investigate this tests were made of a configuration with the tips cut off flush with the base of the body. Results of these tests, presented in figure 5, show that the reduction in static stability of plan form C at lift coefficients above 0.2 was eliminated by removal of the portion of the wing aft of the fuselage base. According to reference 2, this change in wing plan form will result in a reduction of about 10 percent in maximum L/D at hypersonic speeds.

Figure 6 presents results of a series of tests directed toward preventing the reduction in static stability of plan form C by relatively minor changes in geometry. (These tests were made with the single-cone fuselage replaced by the $3/4$ -power fuselage and afterbody shown in figure 1(d). This change had negligible effects on the longitudinal characteristics of the model.) The data presented in figure 6 indicate that it is possible to eliminate the instability at high C_L by filling in the area between the fuselage and the wing trailing edge, and by the addition of simulated landing gear and wheel well doors.

Control effectiveness.- The effectiveness of flap-type controls on the characteristics of plan form C is shown in figures 7(a) and (b). These results show that control effectiveness was maintained throughout the angle-of-attack range and control deflection range investigated.

Lateral Characteristics

Lateral-directional stability.- The static lateral-directional stability characteristics of plan form A are presented in figure 8, and those of plan form C are presented in figure 9. Similar data are presented in figure 10 for plan form C equipped with two vertical fins. A summary plot of the effective dihedral, $C_{l\beta}$, and directional stability, $C_{n\beta}$, as a function of angle of attack with various amounts of wing-tip droop is presented in figures 11 and 12. These results show that, for

most of the configurations, directional stability at zero sideslip increased with increasing angle of attack. As would be expected, effective dihedral decreased and directional stability increased with increasing wing-tip droop.

The directional stability of plan form C with two vertical fins was of the order of two to three times that obtained by drooping the wing tips 60° . Also, the reduction of $C_{n\beta}$ with increasing β obtained for plan form C with drooped tips (shown in fig. 9) was eliminated by the addition of the vertical fins. However, the addition of the vertical fins represents about a 30-percent increase in wetted area of the model so that these improvements in stability characteristics would be obtained only at the expense of significant reductions in high-speed lift-drag ratio.

Lateral-directional control.- The effectiveness of the wing trailing-edge flaps as lateral-directional control devices is shown in figure 13 for wing-tip droop angles of 30° and 60° . These results show no serious deterioration of roll or yaw control with increasing angle of attack. Changing the wing-tip droop from 30° to 60° resulted in a large increase in maximum yaw control and a relatively small decrease in roll power. These results indicate that the use of the wing-tip flaps for roll control would result in favorable yawing-moment inputs, the magnitude of $C_{l\delta_f}/C_{n\delta_f}$ being about 1 with 30° of wing-tip droop, and less than 1/2 with 60° of wing-tip droop. Unpublished analog computer investigations and free-flight tests of dynamically similar models (ref. 3) have shown that the airplane can be flown with these controls alone, although the free-flight tests (made with a model having 45° of wing-tip droop) indicated that the amount of favorable yaw from the ailerons might lead to undesirable flying qualities. Figure 14 presents similar data for plan form C with two vertical fins (see fig. 1(b)), and it is seen that the rudders on the vertical fins provided about three times the directional control provided by the wing-tip flaps.

Landing Considerations

Since this configuration does not obtain its maximum lift coefficient in the angle-of-attack range of interest in the landing approach, the landing approach speed will probably be chosen from considerations of pilot's ability to control rate of sink and avoid reduction in longitudinal stability, and the maximum ground angle of the airplane (about 10° with a conventional length landing gear).

Previous research (refs. 4 and 5) has shown that the ability of a pilot to control the rate of sink of an airplane is related to the flight speed for minimum glide angle. As the speed is reduced below that for

minimum glide angle, the ability to control rate of sink generally is also reduced. A plot of glide angle as a function of flight speed is presented in figure 15 for a hypothetical airplane having a configuration similar to plan form C and a wing loading of 20 pounds per square foot. (This value of wing loading was selected from considerations of high-speed, high-altitude flight as well as from landing requirements.) Also shown in this figure for comparison are curves for the X-15 and X-4 airplanes (from the data presented in refs. 6 and 7, respectively). It is seen that the glide-angle versus flight-speed curves of the arrowhead configuration and the X-15 are quite similar, from which it might be inferred to a first approximation that control of rate of sink of these two configurations would be comparable. The glide-angle versus flight-speed characteristics of the X-4 airplane are of interest because a fairly thorough flight investigation of the landing approach characteristics of this airplane has been made (ref. 6). While landings were made with the X-4 airplane for values of glide angle and speed of the same order as the arrowhead and X-15 configurations, it should be noted that the speed for minimum glide angle was never approached in the X-4 landing approaches, and that, in general, the shape of the glide-angle versus speed curve for the X-4 suggests a much higher level of speed-altitude stability than do those for the arrowhead or X-15 configurations.

Plots of glide angle, angle of attack, and attitude angle as a function of steady-state sinking speed are shown in figure 16 for the arrowhead-wing configuration. It is seen that, at the minimum sinking speed, control of steady-state rate of sink with either angle of attack or airplane attitude is completely lost.

Figure 17 shows computed power-off landing flare paths of the arrowhead configuration and an actual landing flare path for the X-4 airplane (obtained from the data presented in ref. 6). The theory of reference 8 was used to compute the flare path for the arrowhead configuration with the assumption that the lift coefficient used in the flare did not exceed that for maximum L/D . This restriction on lift coefficient limits the angle of attack used in the flare to values below those for which the longitudinal stability deteriorates, and also limits the angle of attack at the end of the flare to a value less than the assumed tail bumping attitude of 10° . It was also assumed that the normal acceleration used in the flare varied as $\sin^2 \pi t/t_2$ (where t is the time from the start of the flare and t_2 is the time required to complete the flare) and that the maximum normal acceleration used was 1.75g. Other normal-acceleration programs would, of course, give different flare paths, but it is believed the one shown gives an indication of the main features of the flare. The computations indicate that, as with the X-4 airplane, the flare would be started at an altitude of about 400 to 500 feet and would be essentially completed at an altitude of 50 feet. The horizontal distance estimated to complete the flare is about 3200 feet, and the flight speed decreases from 218 knots at the start of the flare to 173 knots at the end of the flare.

In summary, these results indicate that the power-off landing of such configurations will be a difficult task to be undertaken only by skillful pilots and under ideal conditions. The main source of difficulty is the high power-off rate of sink resulting from the low values of maximum L/D inherent in these low-aspect-ratio configurations. If power were used in the landing approach to reduce the rate of sink to a more reasonable value, it is believed that landings could be accomplished in a more conventional fashion.

CONCLUDING REMARKS

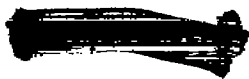
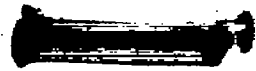
The following low-speed longitudinal aerodynamic characteristics of arrowhead-wing configurations will be of particular importance in the landing of such aircraft: (1) low values of lift-curve slope, (2) low values of maximum lift-drag ratio, and (3) reduction in static stability at high angles of attack. Low values of lift-curve slope and lift-drag ratio are inherent in low-aspect-ratio plan forms of this type, and there is little possibility of significantly increasing either by minor fixes. Preliminary results indicate that the reduction in static stability can at least be reduced or possibly eliminated by relatively minor configuration changes. It is anticipated that power-off landings of these configurations will require ideal conditions and skilled piloting, primarily because of the high rate of sink. The use of power to reduce the rate of sink prior to the flare should allow landings to be made in a more conventional manner.

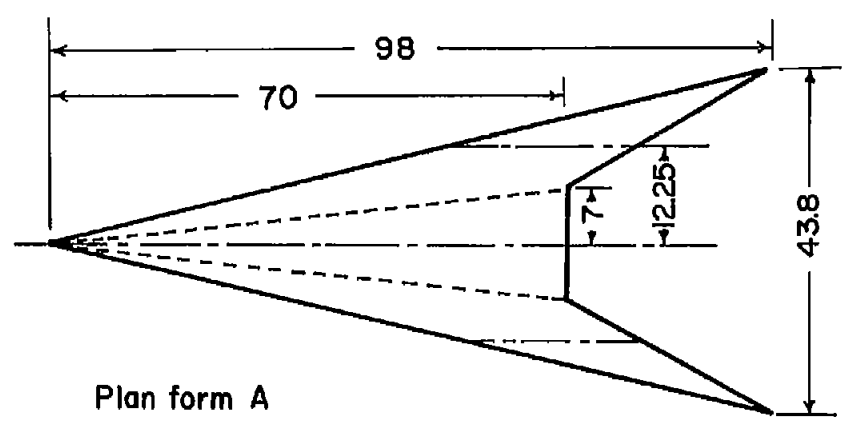
The configurations investigated were generally both laterally and directionally stable at zero sideslip over an angle-of-attack range from 4° to 20° . The lateral and directional stability was, of course, strongly affected by the amount of wing-tip droop. Trailing-edge flaps at the wing tips were capable of supplying both roll and yaw control inputs, and preliminary analysis indicates that it should be possible to fly such a configuration as a two-control airplane. However, if this were done, a careful selection of wing-tip droop would have to be made to obtain the most favorable combination of $C_{l\delta_f}$, $C_{n\delta_f}$, $C_{l\beta}$, and $C_{n\beta}$. The use of vertical fins near the wing tips increased the directional stability and essentially eliminated the cross-coupling between the roll and yaw controls.

Ames Aeronautical Laboratory
National Advisory Committee for Aeronautics
Moffett Field, Calif., June 3, 1958

REFERENCES

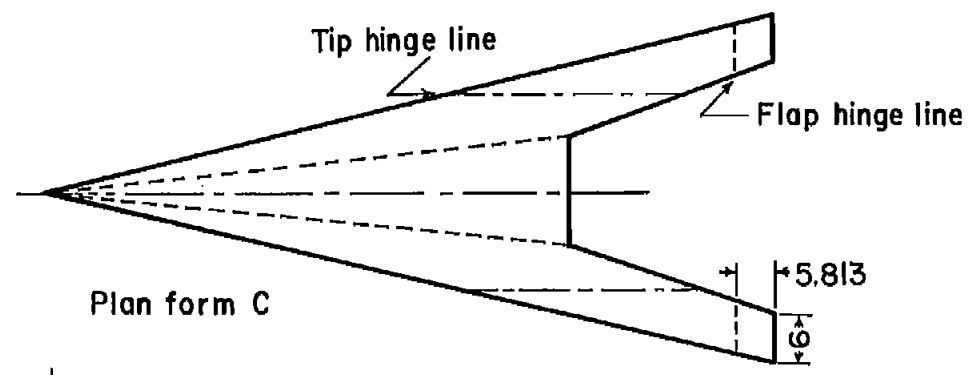
1. Eggers, A. J., Jr., and Syvertson, Clarence A.: Aircraft Configurations Developing High Lift-Drag Ratios at High Supersonic Speeds. NACA RM A55L05, 1956.
2. Syvertson, Clarence A., Wong, Thomas J., and Gloria, Hermilo R.: Additional Experiments With Flat-Top Wing-Body Combinations at High Supersonic Speeds. NACA RM A56L11, 1957.
3. Moul, Martin T., and Paulson, John W.: Dynamic Lateral Behavior of High-Performance Aircraft. NACA RM L58E16, 1958.
4. White, Maurice D., Schlaff, Bernard A., and Drinkwater, Fred J., III.: A Comparison of Flight-Measured Carrier-Approach Speeds With Values Predicted by Several Different Criteria for 41 Fighter-Type Airplane Configurations. NACA RM A57L11, 1958.
5. Neumark, S.: Problems of Longitudinal Stability Below Minimum Drag Speed, and Theory of Stability Under Constraint. British A.R.C. R. & M. No. 2983, 1957. (Also available as R.A.E. Aero. 2504, July 1953)
6. Stillwell, Wendell H.: Results of Measurements Made During the Approach and Landing of Seven High-Speed Research Airplanes. NACA RM H54K24, 1955.
7. Boisseau, Peter C.: Investigation of the Low-Speed Stability and Control Characteristics of a 1/7-Scale Model of the North American X-15 Airplane. NACA RM L57D09, 1957.
8. Fusfeld, Robert D.: A Method of Calculating the Landing Flare Path of an Airplane. Aero. Eng. Rev., vol. 10, no. 2, Feb. 1951, pp. 25-30.



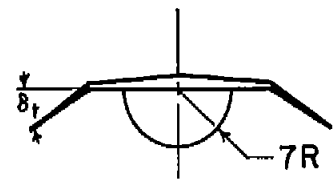
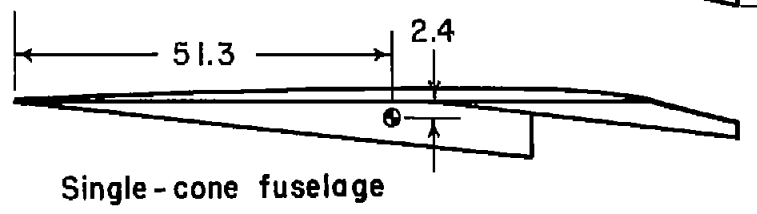


All dimensions in inches

Plan form A
 $AR = 1.4$
 $t/c = .0175$
 $\Delta_{LE} = 77.38^\circ$
 $S = 9.3 \text{ ft}^2$
 Airfoil section-single wedge

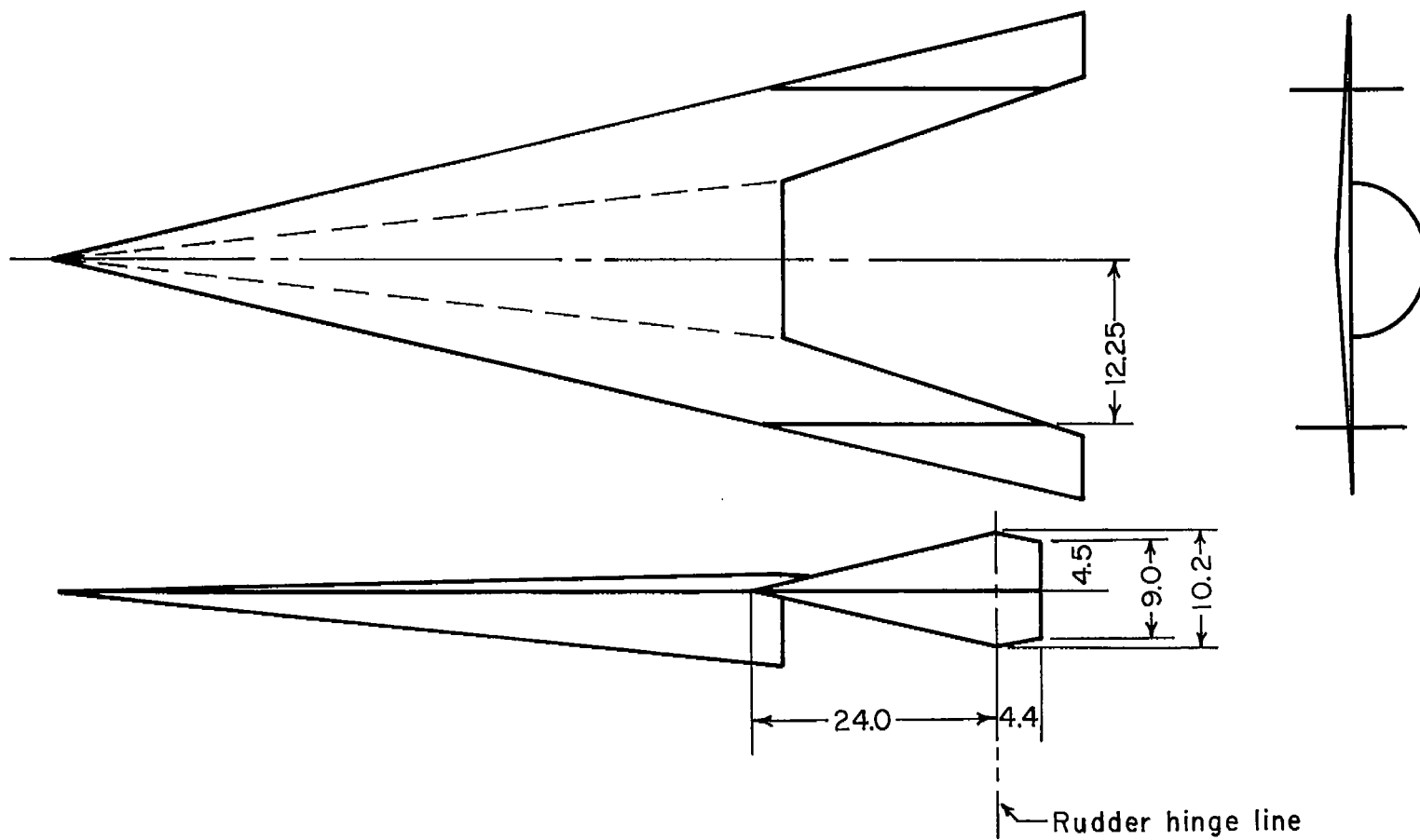


Plan form C
 $AR = 1.3$
 $t/c = .0175$
 $\Delta_{LE} = 77.38^\circ$
 $S = 10.3 \text{ ft}^2$
 Airfoil section-single wedge



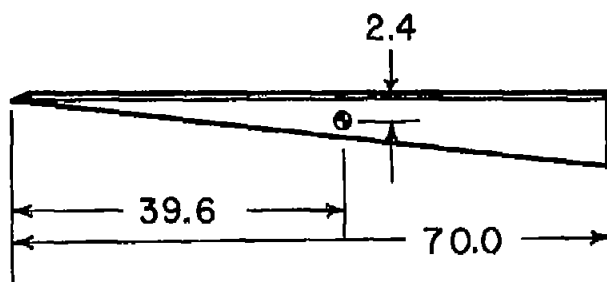
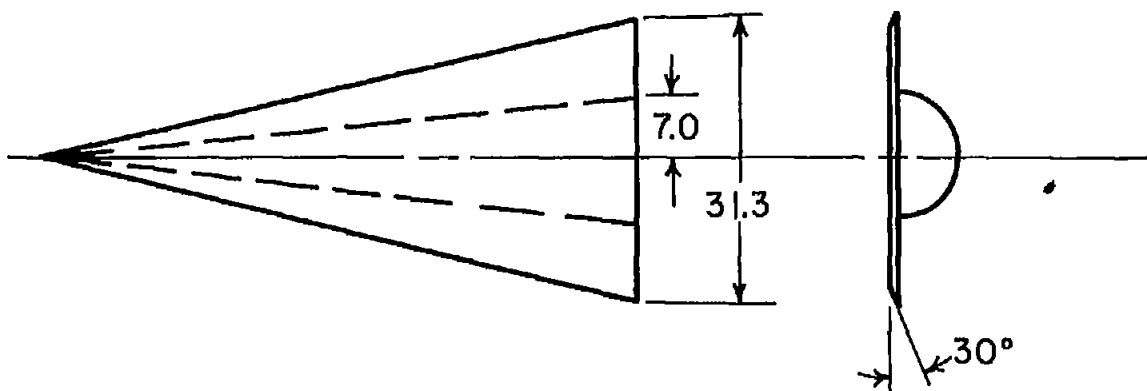
(a) Details of plan forms A and C.

Figure 1.- Geometric characteristics of models.



(b) Vertical-fin configuration.

Figure 1.- Continued.



$$AR = .89$$

$$t/c = .037$$

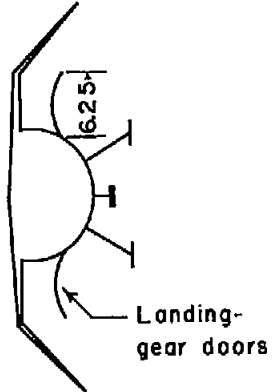
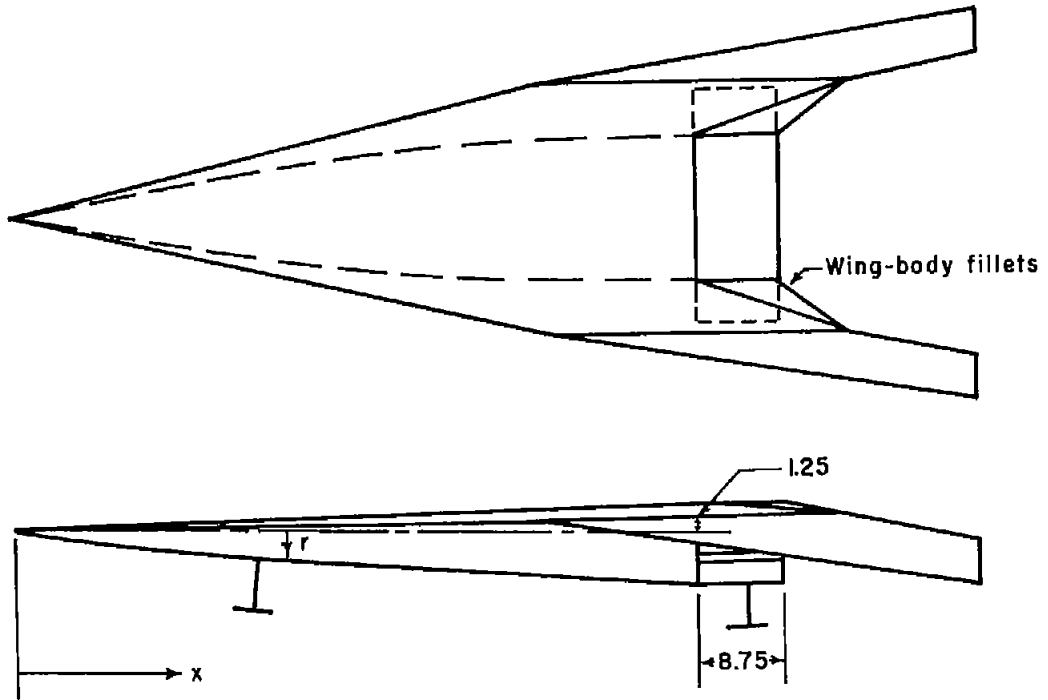
$$\Delta_{LE} = 77.4^\circ$$

$$S = 7.6 \text{ ft}^2$$

Airfoil section - constant thickness
with beveled leading edge

(c) Details of triangular wing.

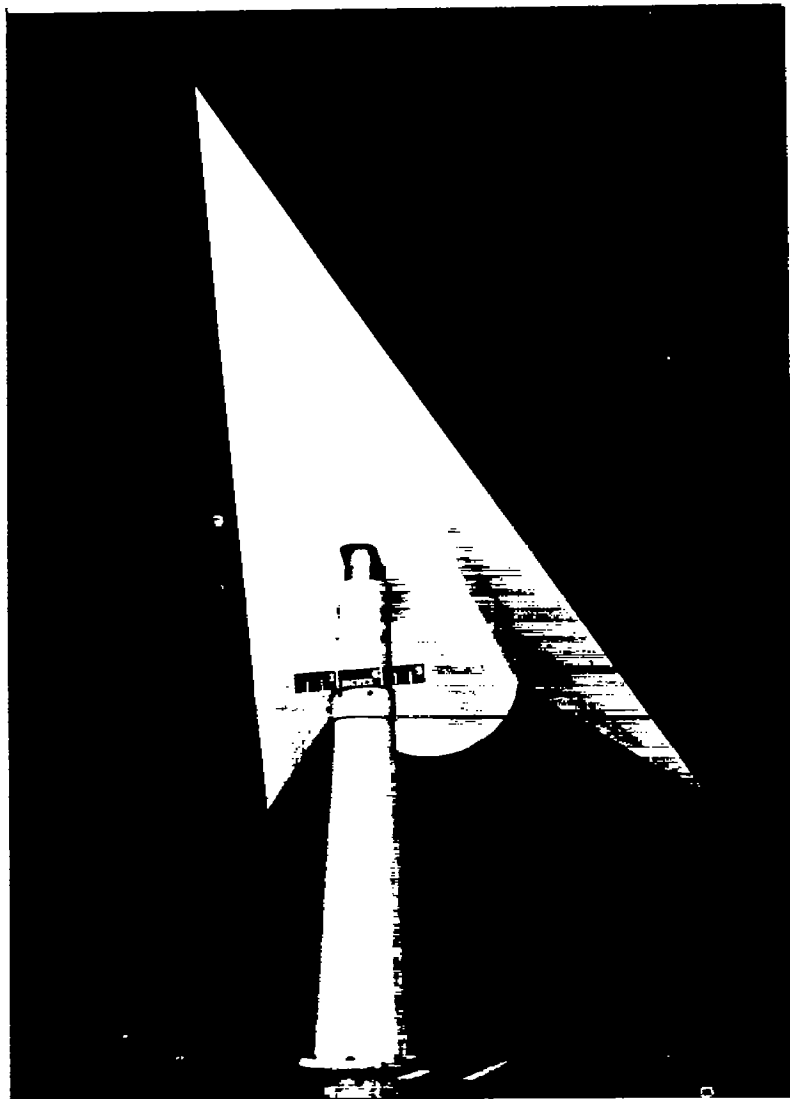
Figure 1.- Continued.



$$r = 6.25(x/4)^{3/4}$$

(d) Landing approach configuration (with 3/4-power fuselage and afterbody).

Figure 1.- Concluded.



A-21407

Figure 2.- Model of plan form A installed in Ames 7- by 10-foot wind tunnel.

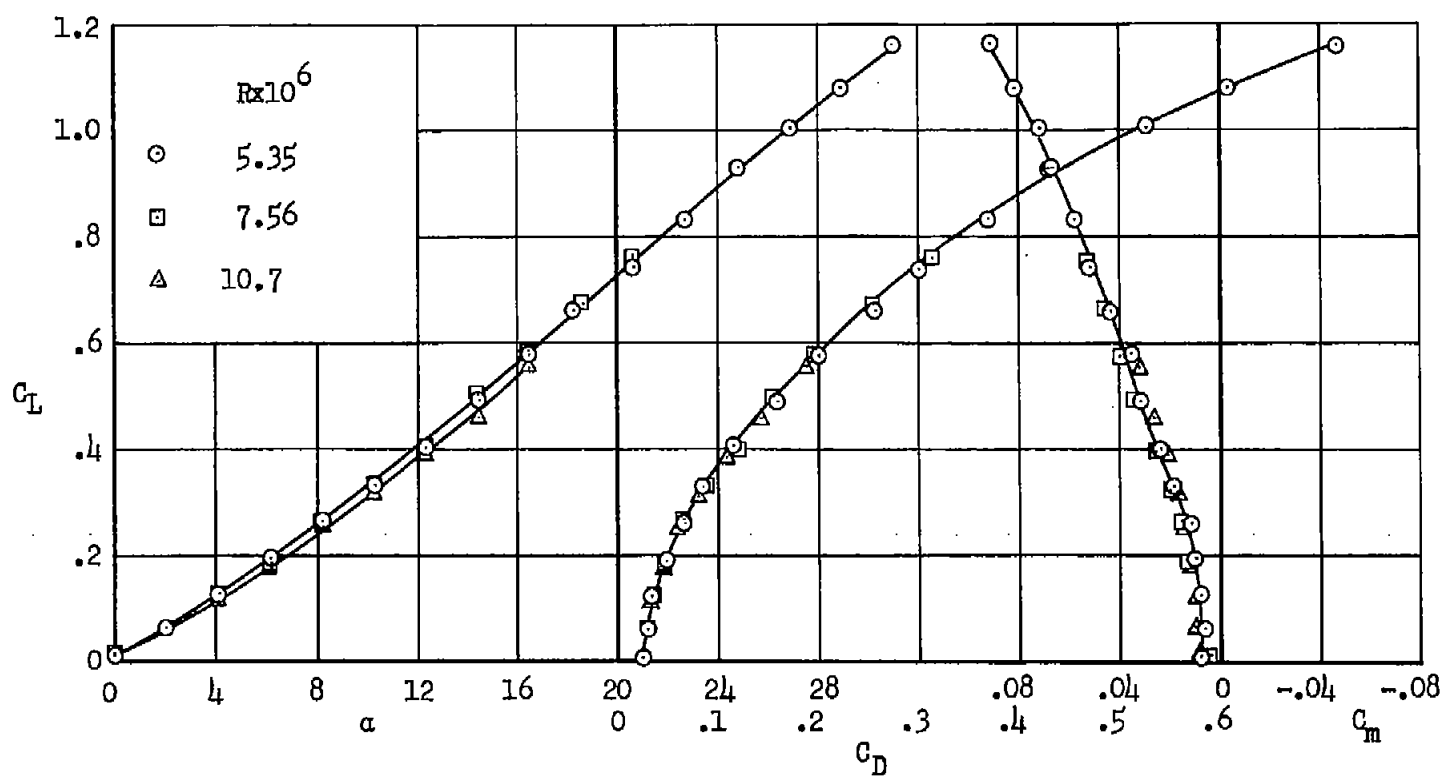
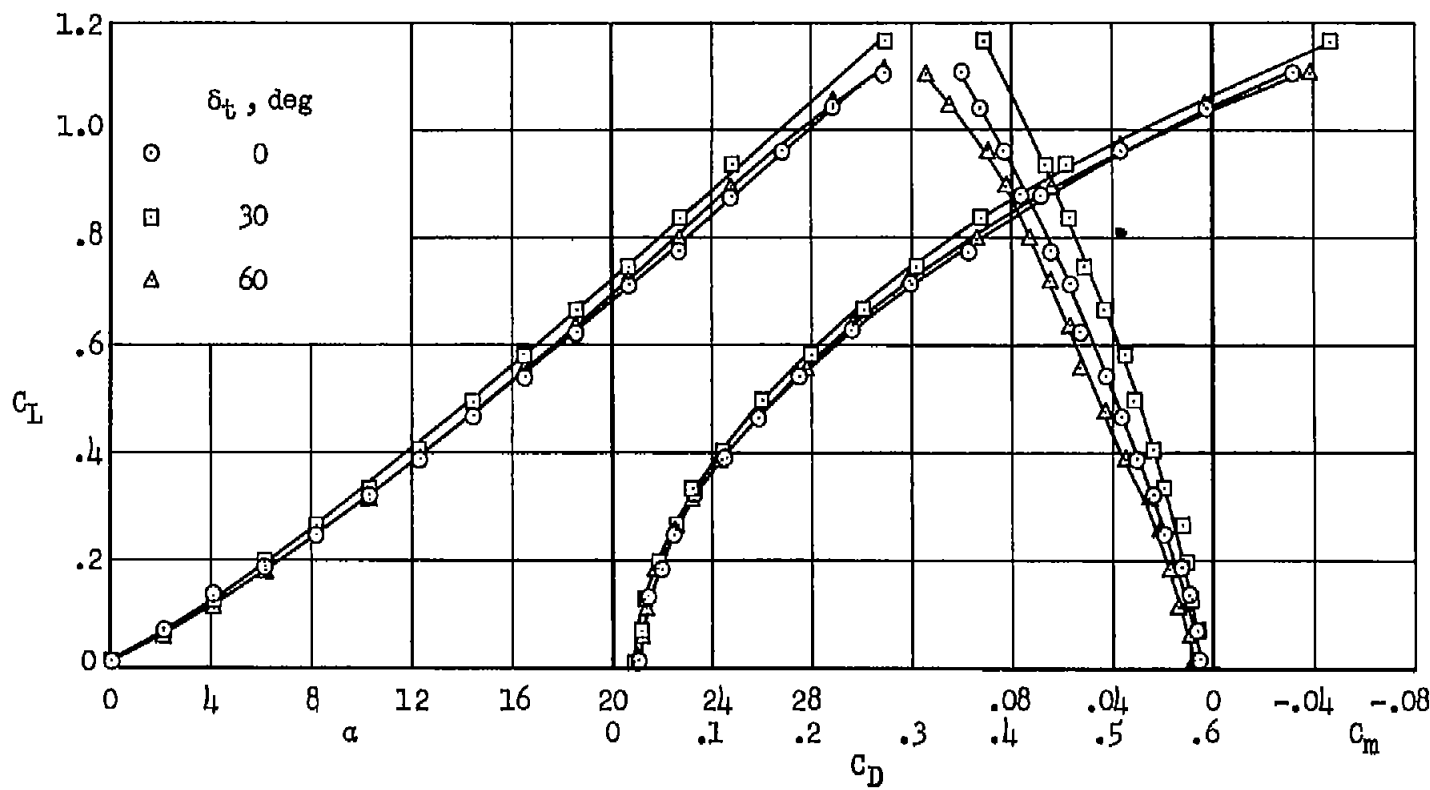
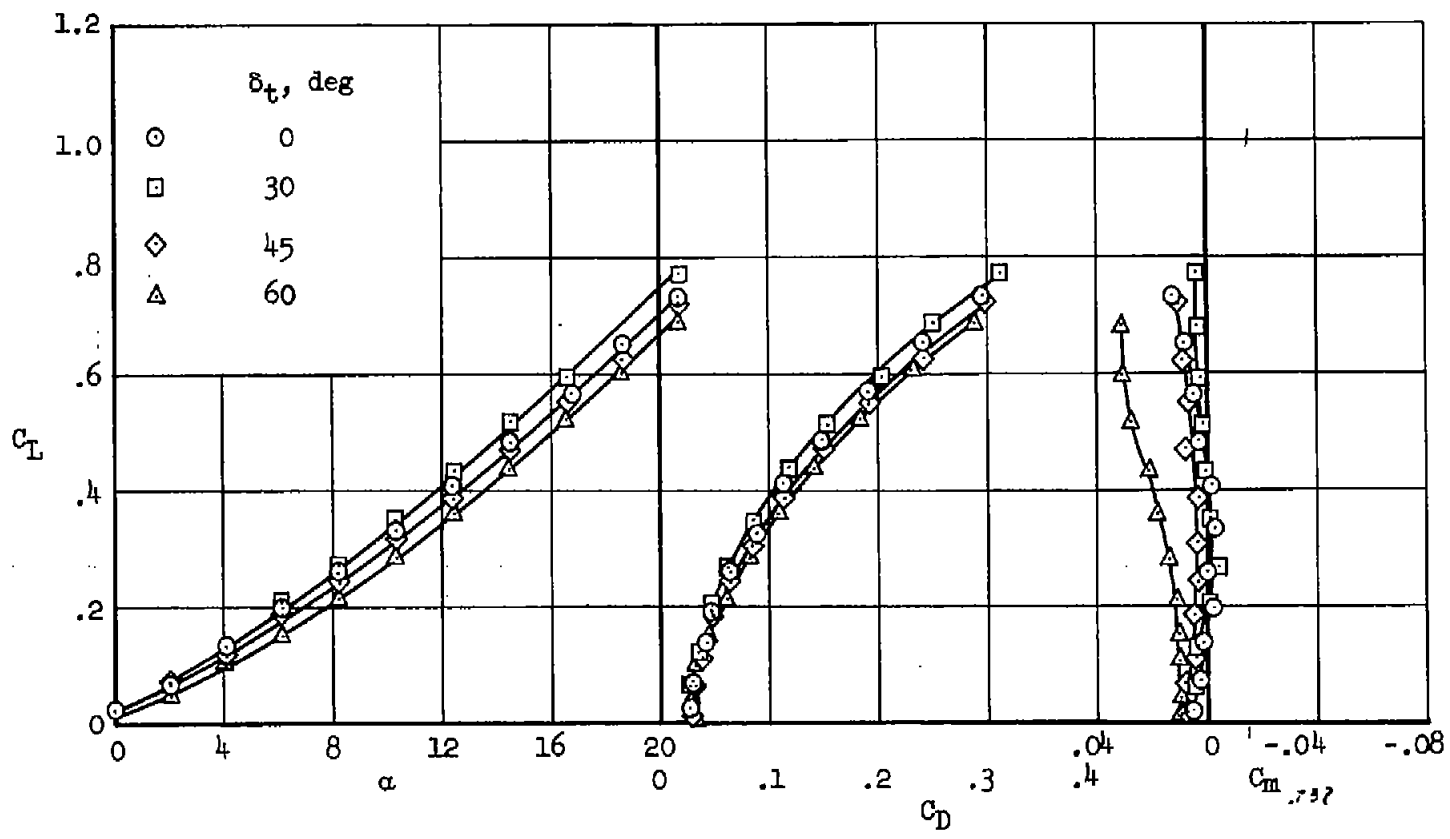


Figure 3.- The effects of Reynolds number on the longitudinal characteristics of plan form A; $\delta_t = 30^\circ$.



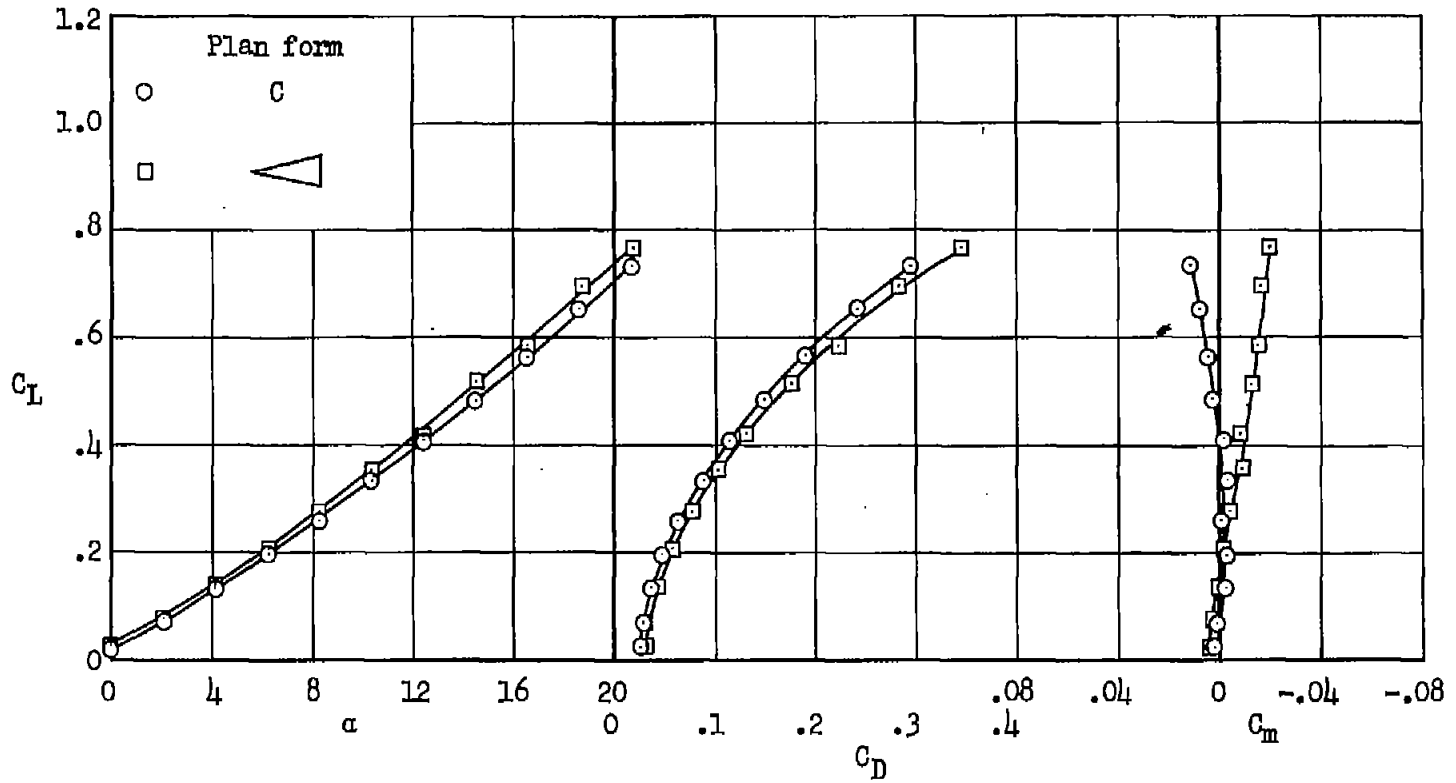
(a) Plan form A.

Figure 4.- Effects of wing-tip droop on longitudinal characteristics.



(b) Plan form C.

Figure 4.- Concluded.



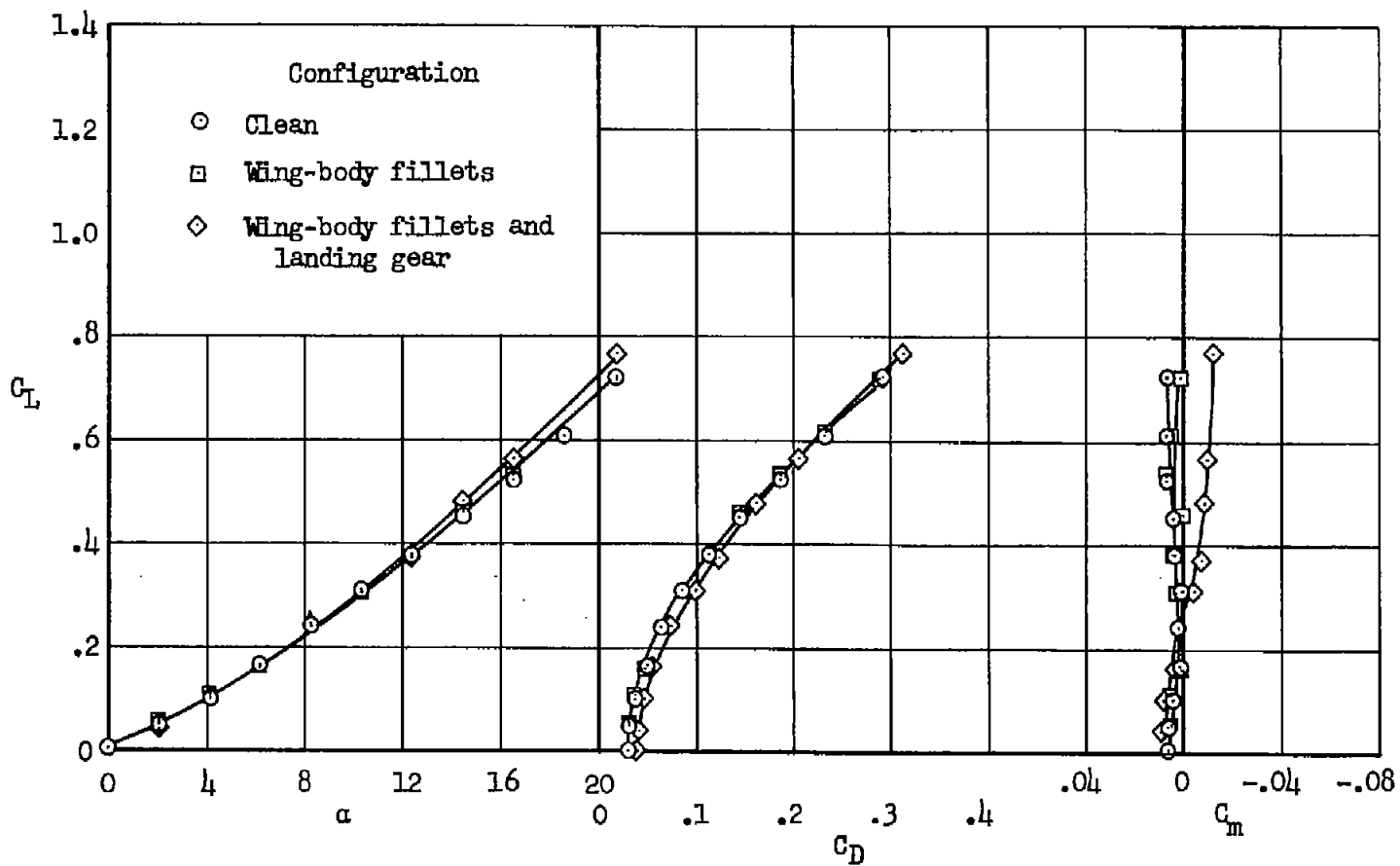
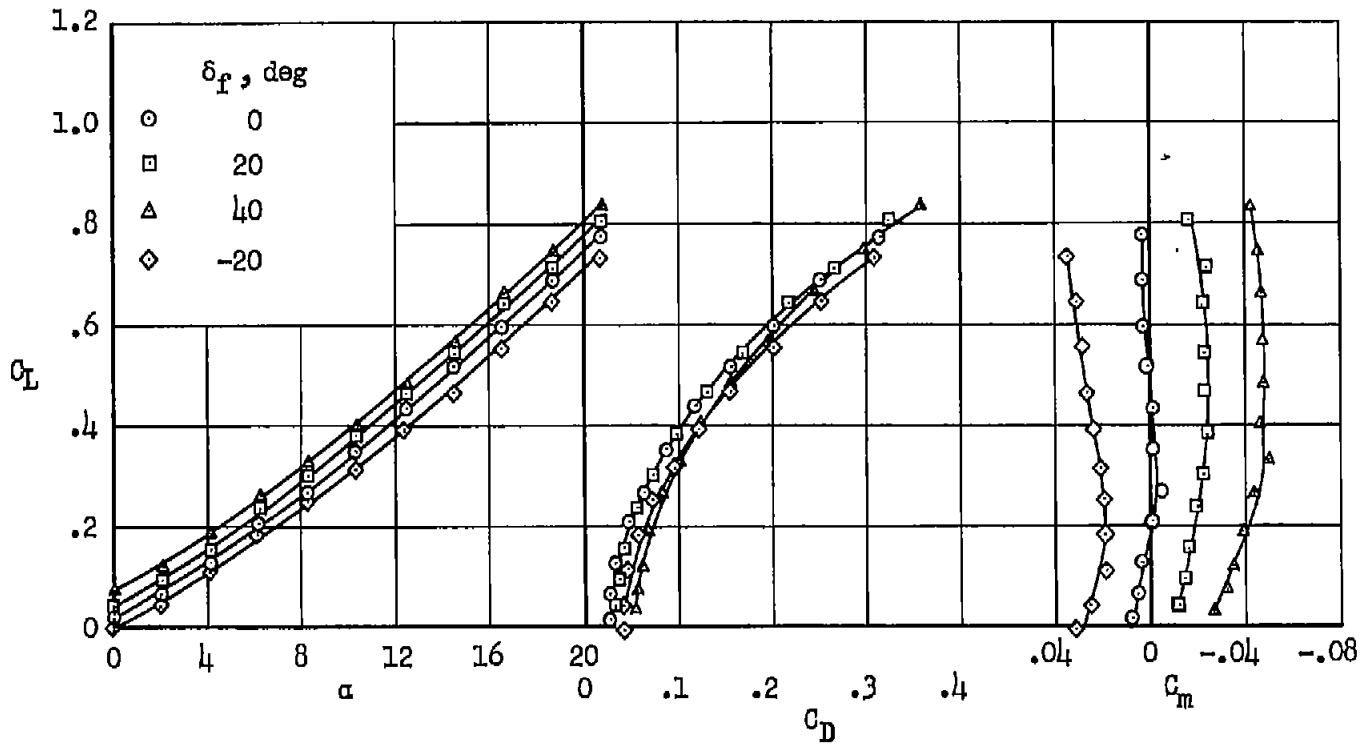
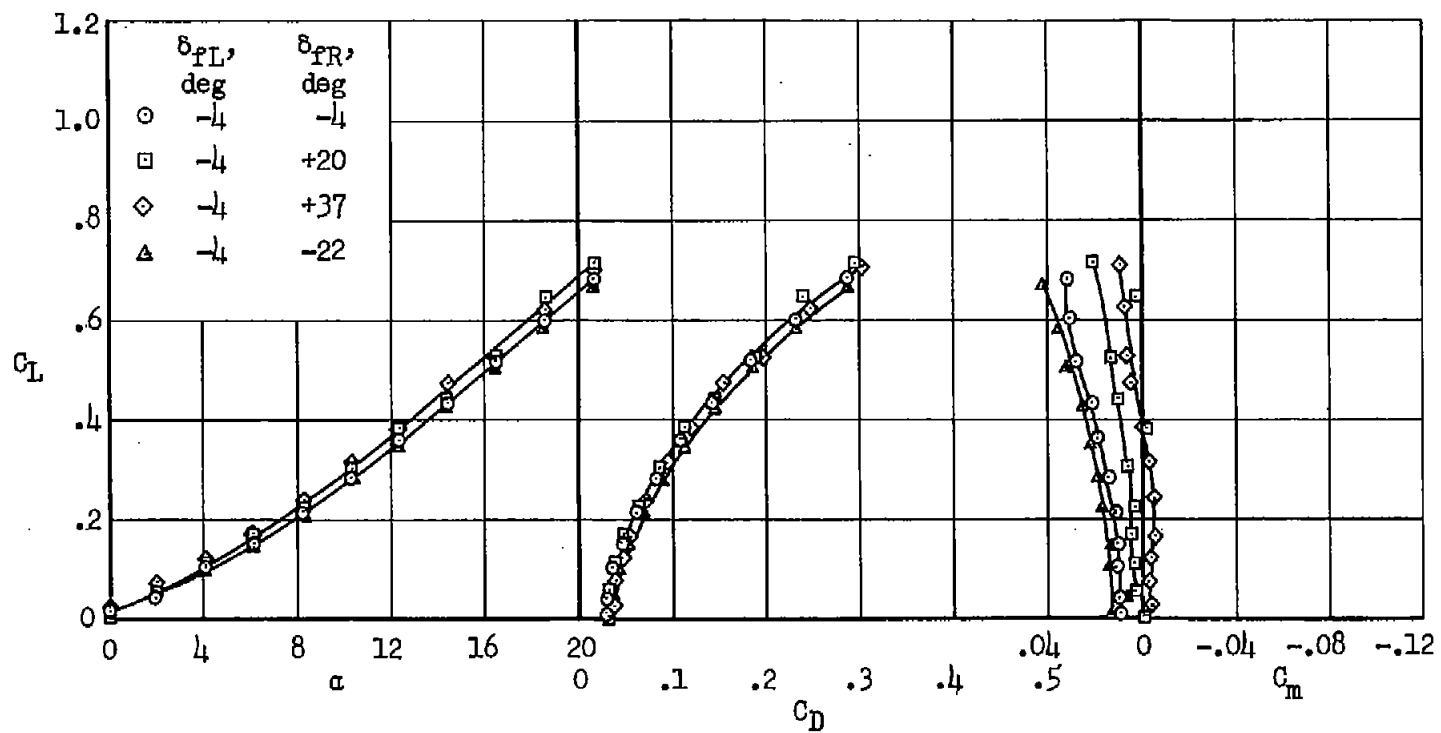


Figure 6.- Effects of adding wing-body fillets and landing gear on longitudinal stability; plan form C with 3/4-power fuselage and afterbody, $\delta_t = 45^\circ$.



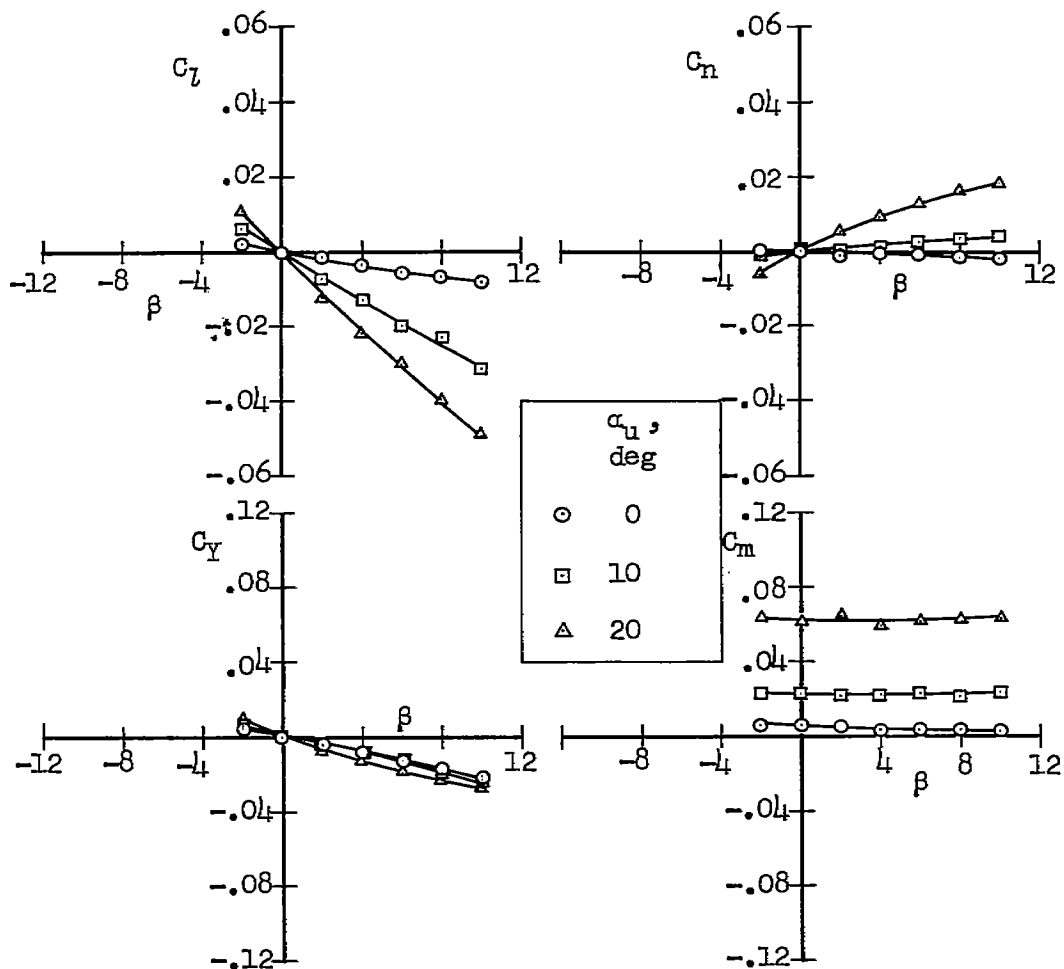
(a) $\delta_t = 30^\circ$

Figure 7.- Effects of flap deflection on the longitudinal characteristics of plan form C.



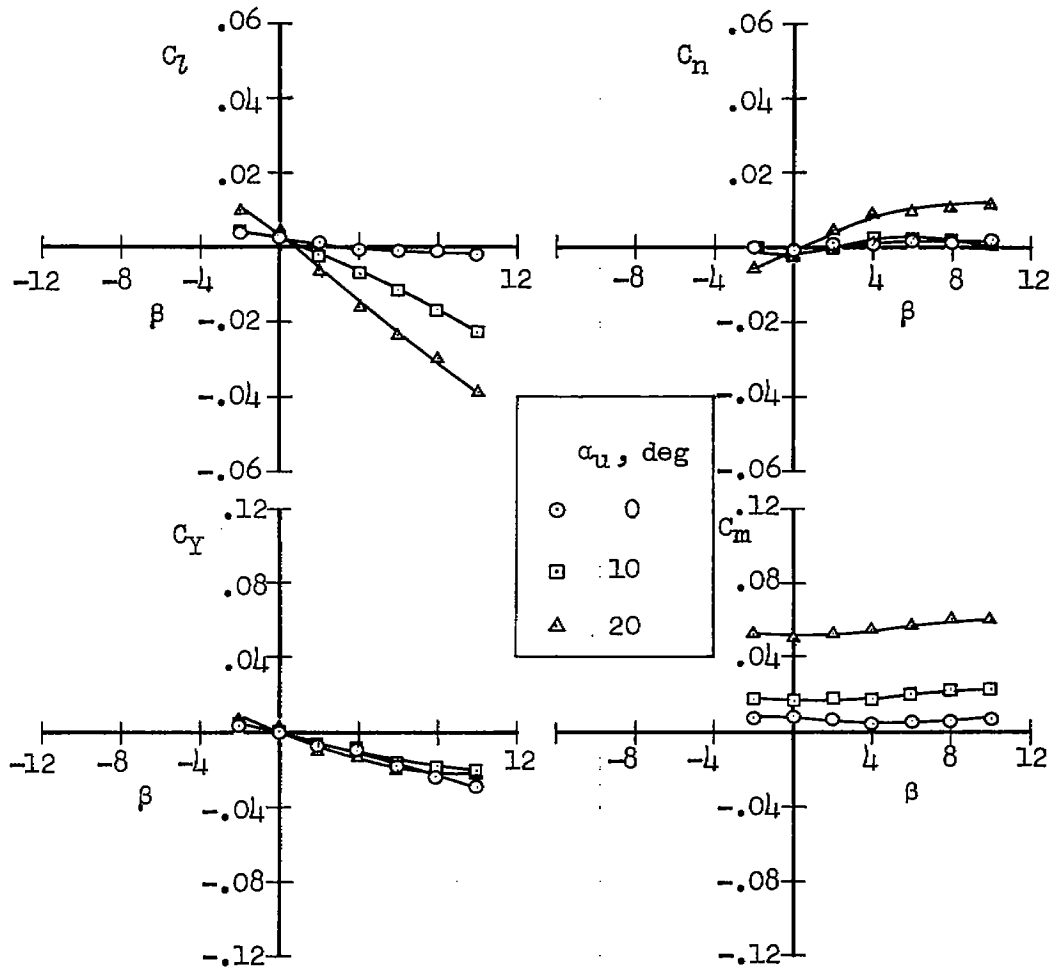
(b) $\delta_t = 60^\circ$

Figure 7.- Concluded.



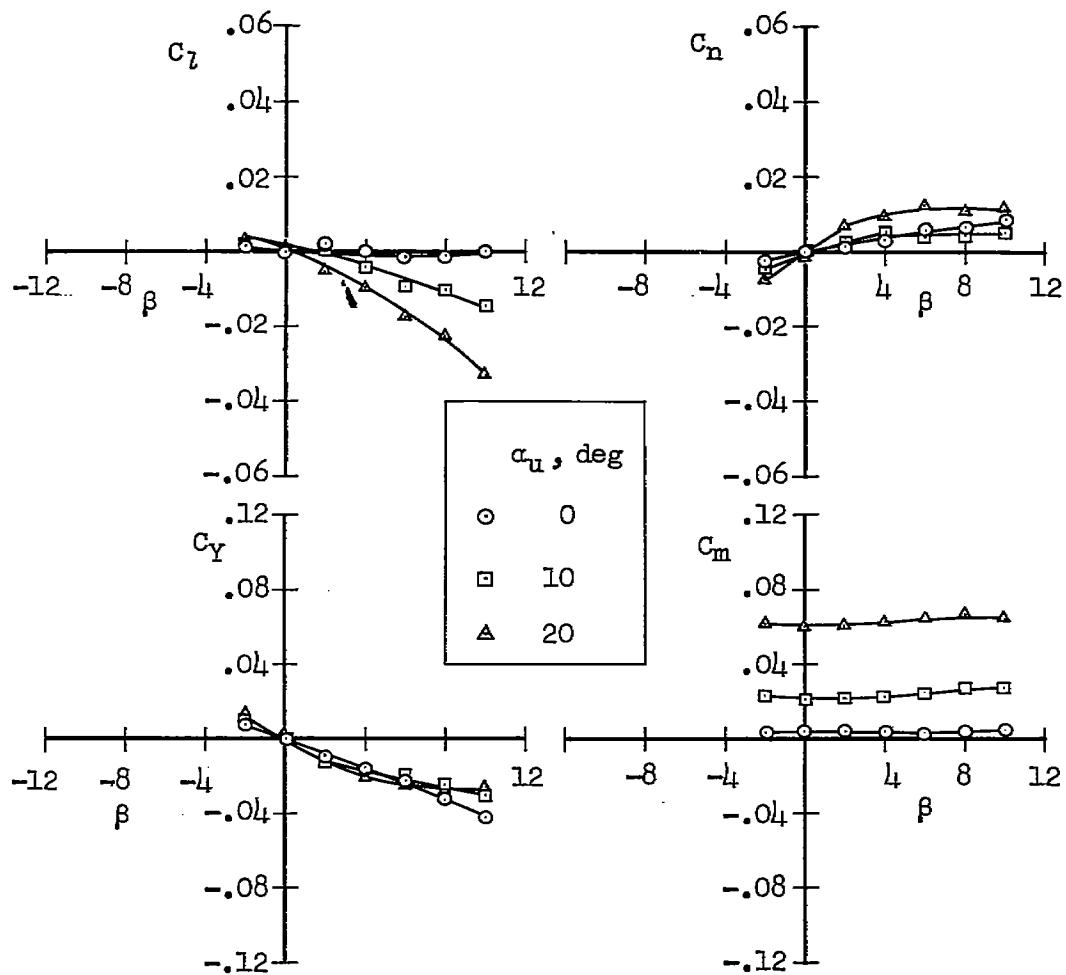
(a) $\delta_t = 0^\circ$

Figure 8.- Lateral characteristics of plan form A.



(b) $\delta_t = 30^\circ$

Figure 8.- Continued.



(c) $\delta_t = 60^\circ$

Figure 8.- Concluded.

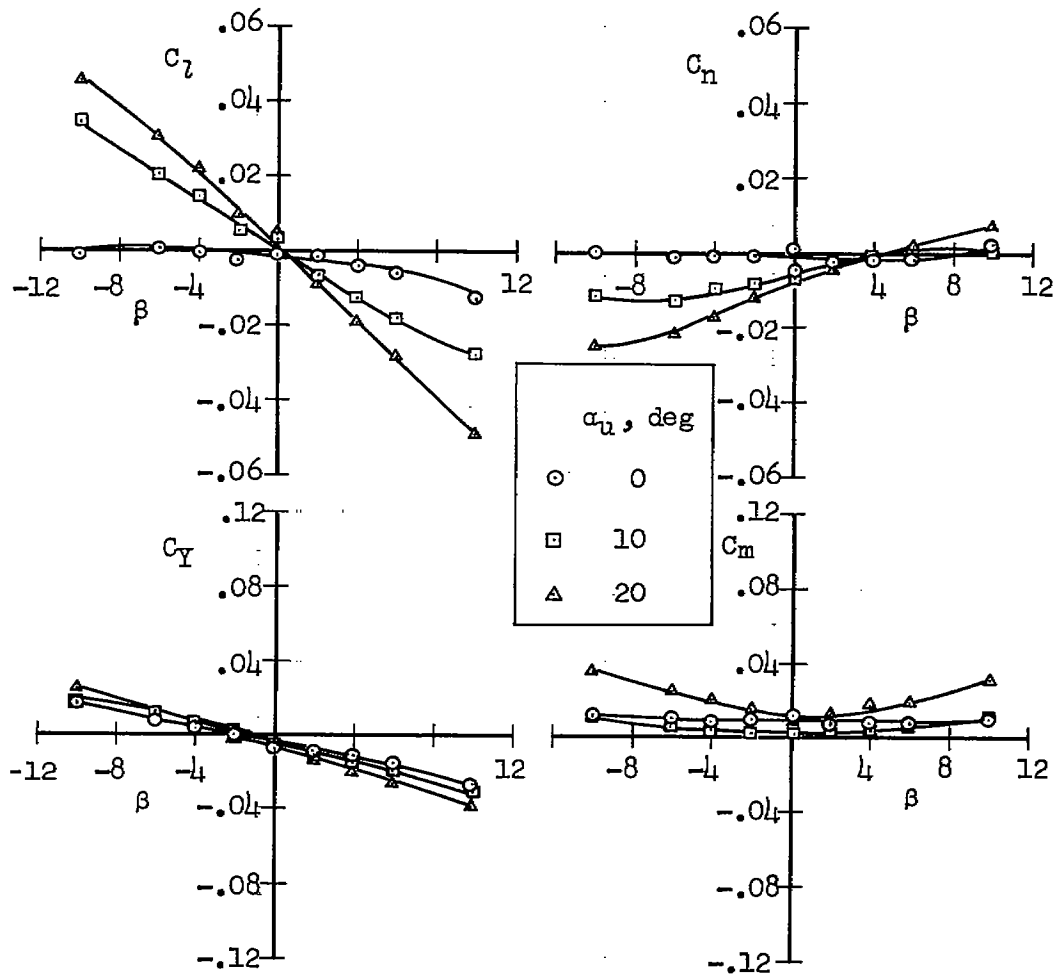
(a) $\delta_t = 0^\circ$

Figure 9.- Lateral characteristics of plan form C.

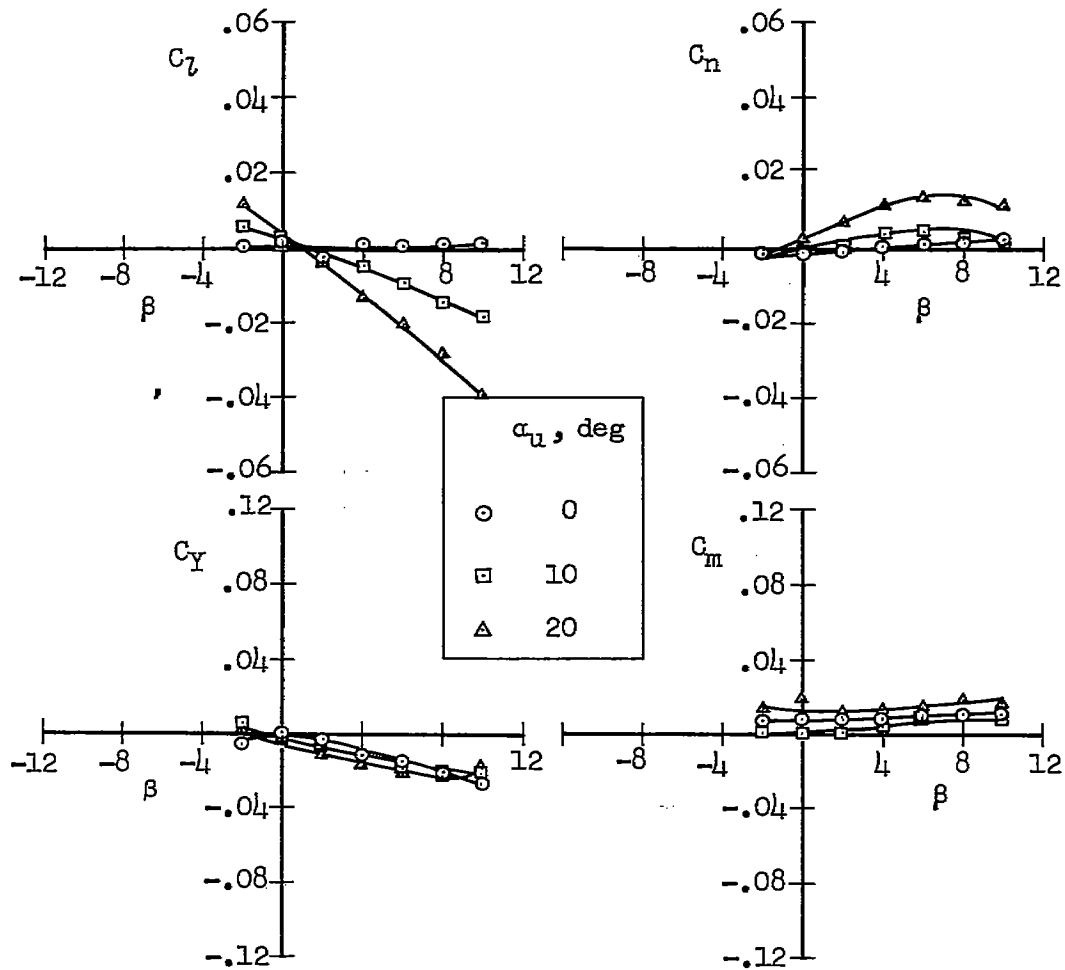
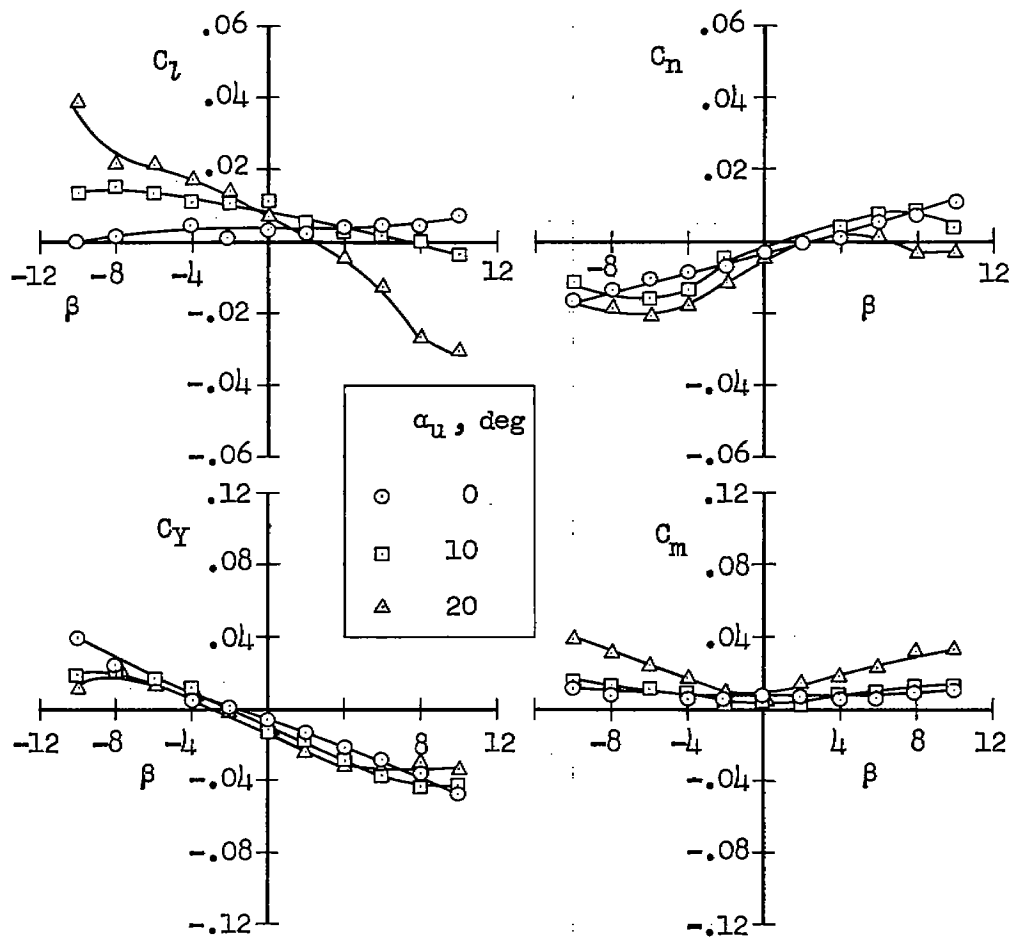
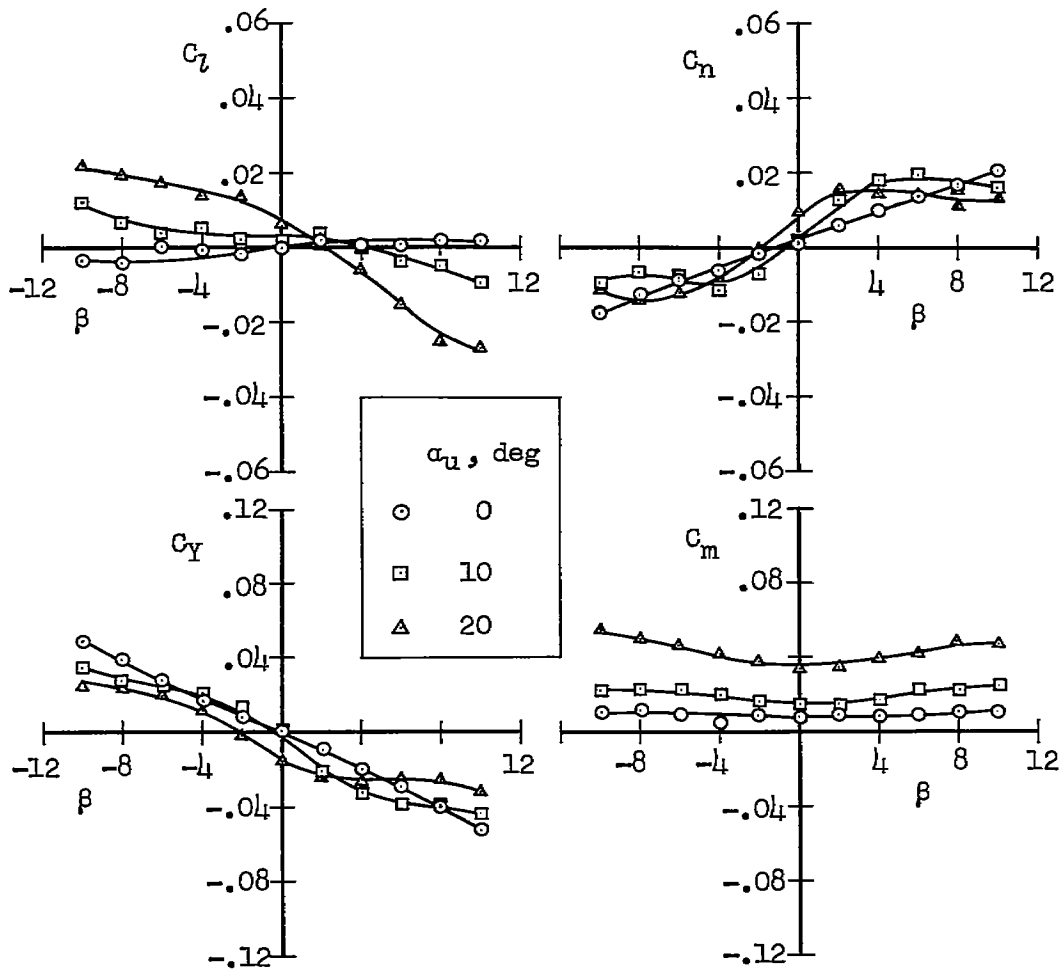
(b) $\delta_t = 30^\circ$

Figure 9.- Continued.



(c) $\delta_t = 45^\circ$

Figure 9.- Continued.



(d) $\delta_t = 60^\circ$

Figure 9.- Concluded.

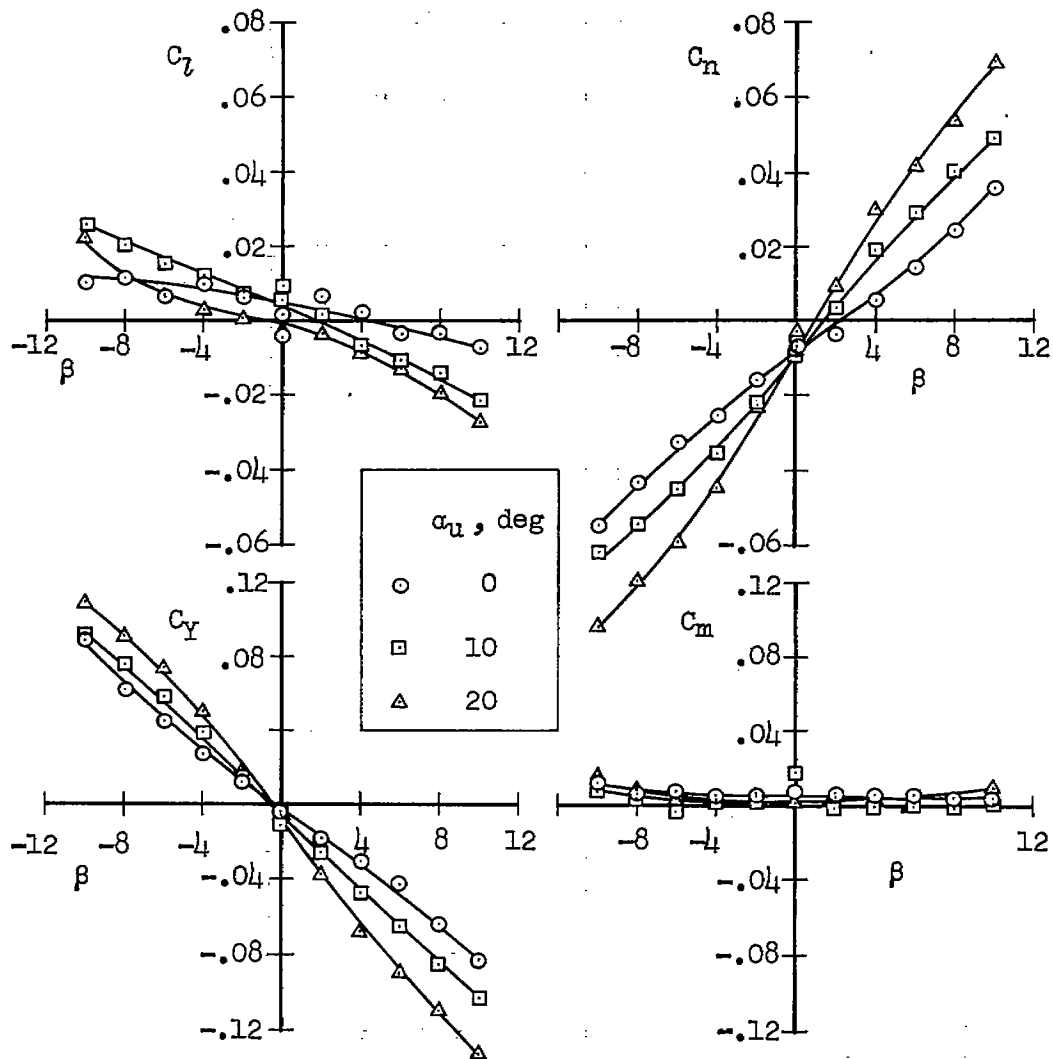


Figure 10.- Lateral characteristics of plan form C with twin vertical fins; $\delta_t = 0^\circ$.

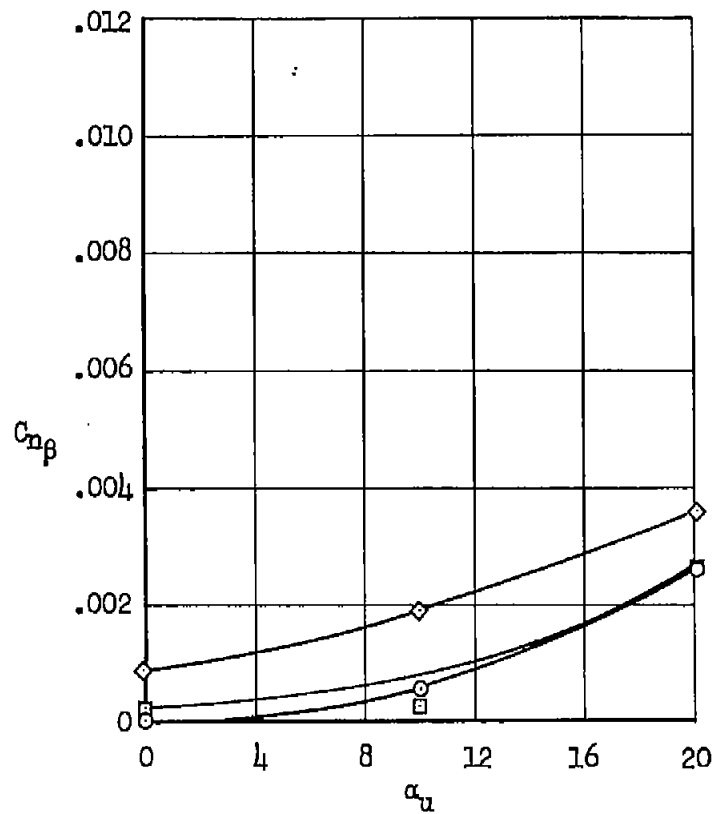
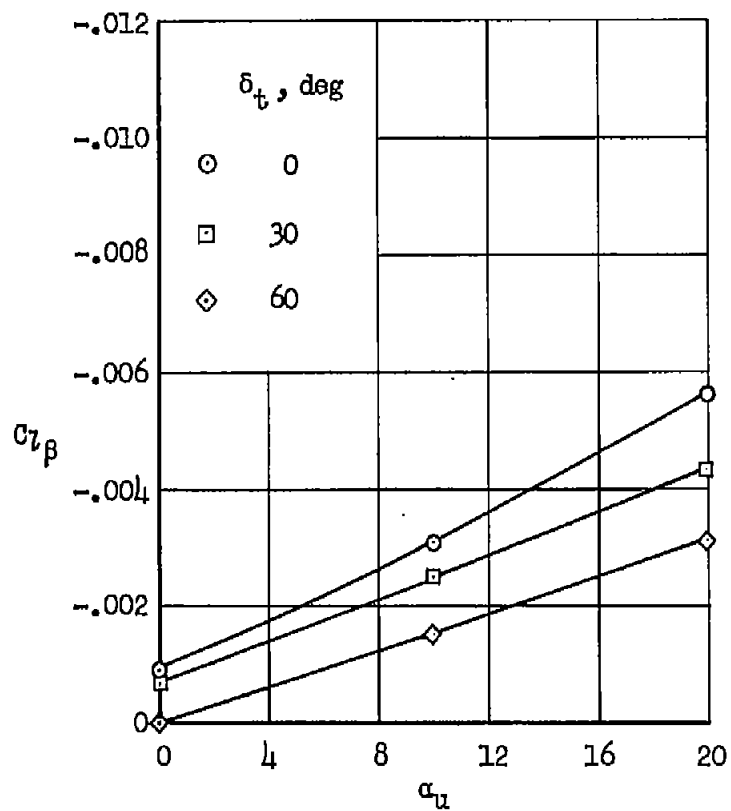


Figure 11.- Variation of $C_{l\beta}$ and $C_{n\beta}$ with α_u and δ_t ; plan form A.

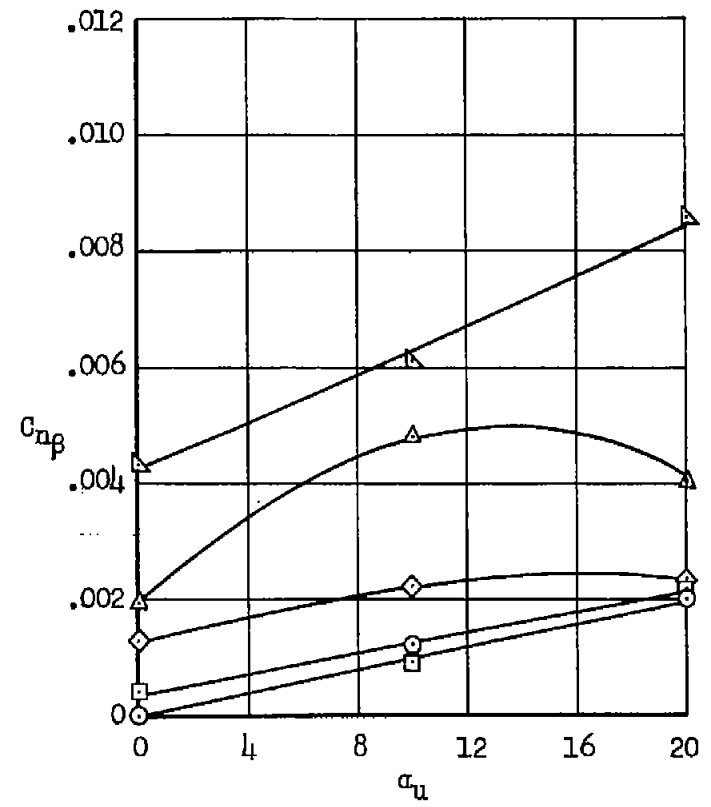
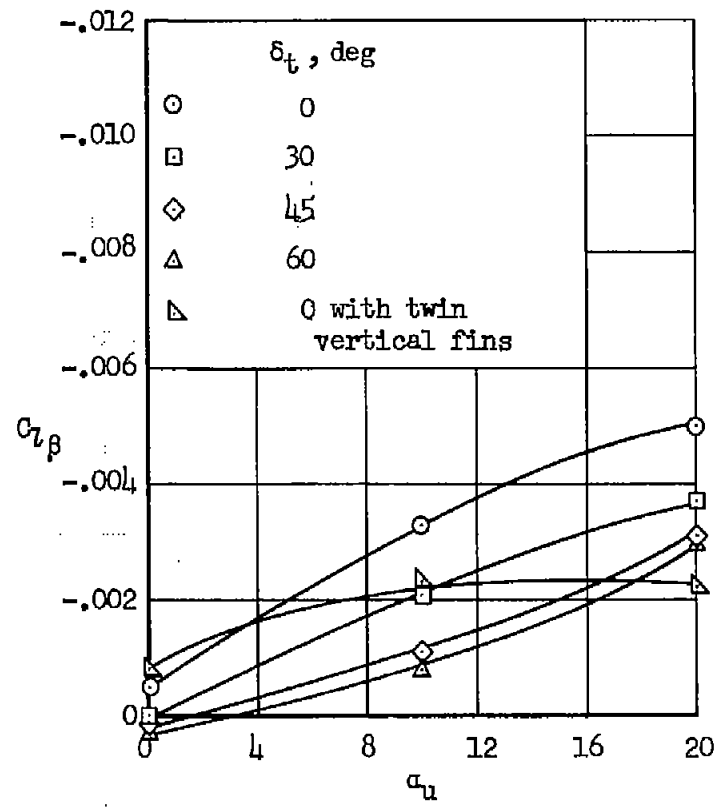
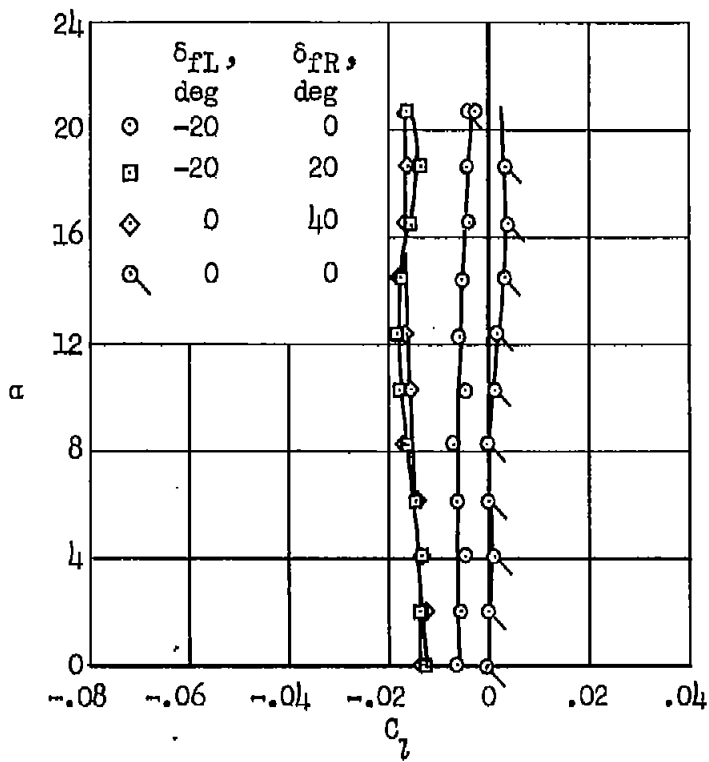
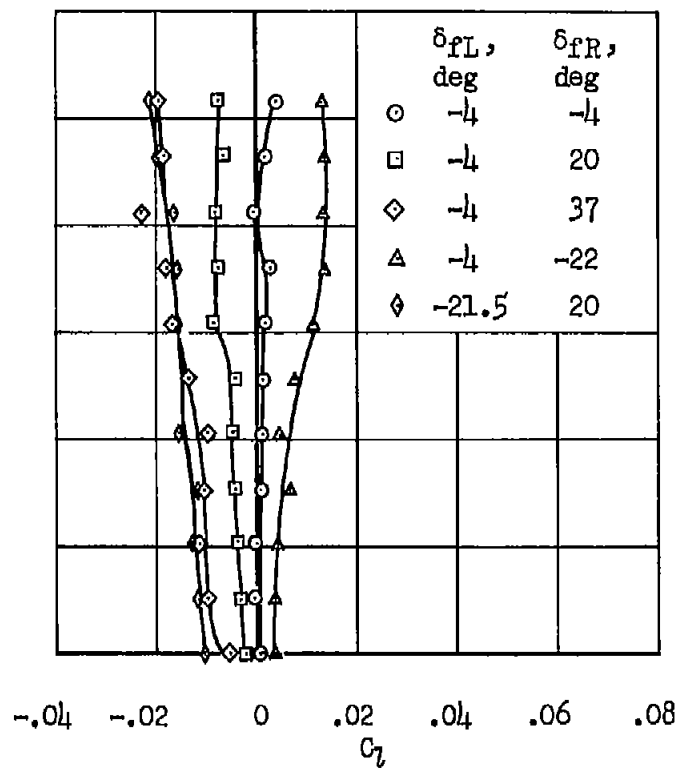


Figure 12.- Variation of $C_{l\beta}$ and $C_{n\beta}$ with α_u and δ_t ; plan form C.

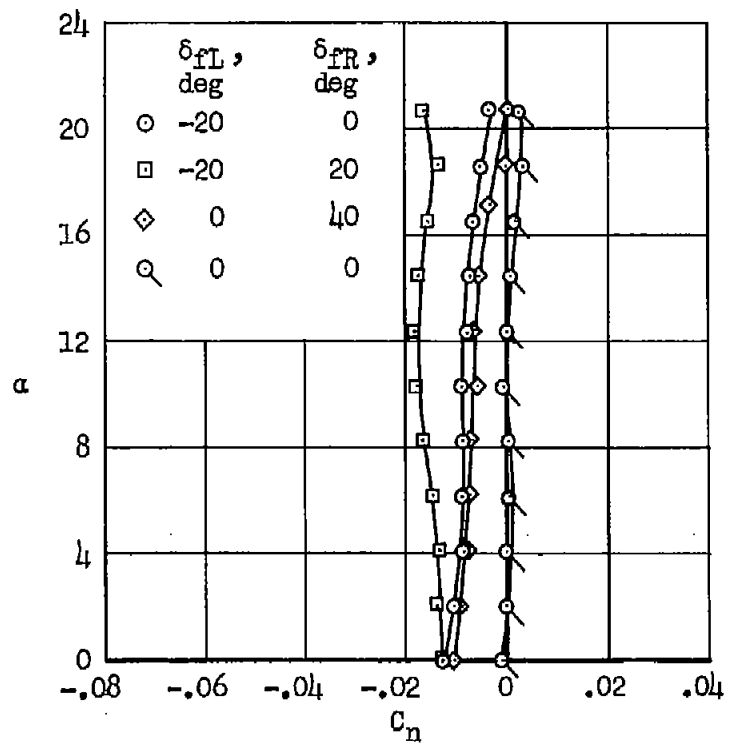


(a) $\delta_t = 30^\circ$

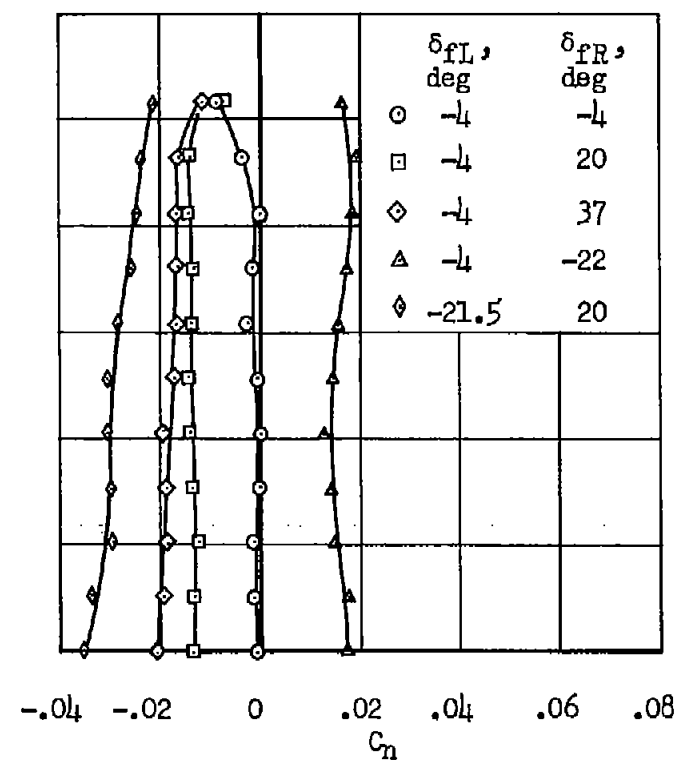


(b) $\delta_t = 60^\circ$

Figure 13.- Variation of C_l and C_n with α_u and δ_f ; plan form C.



(c) $\delta_t = 30^\circ$



(d) $\delta_t = 60^\circ$

Figure 13.- Concluded.

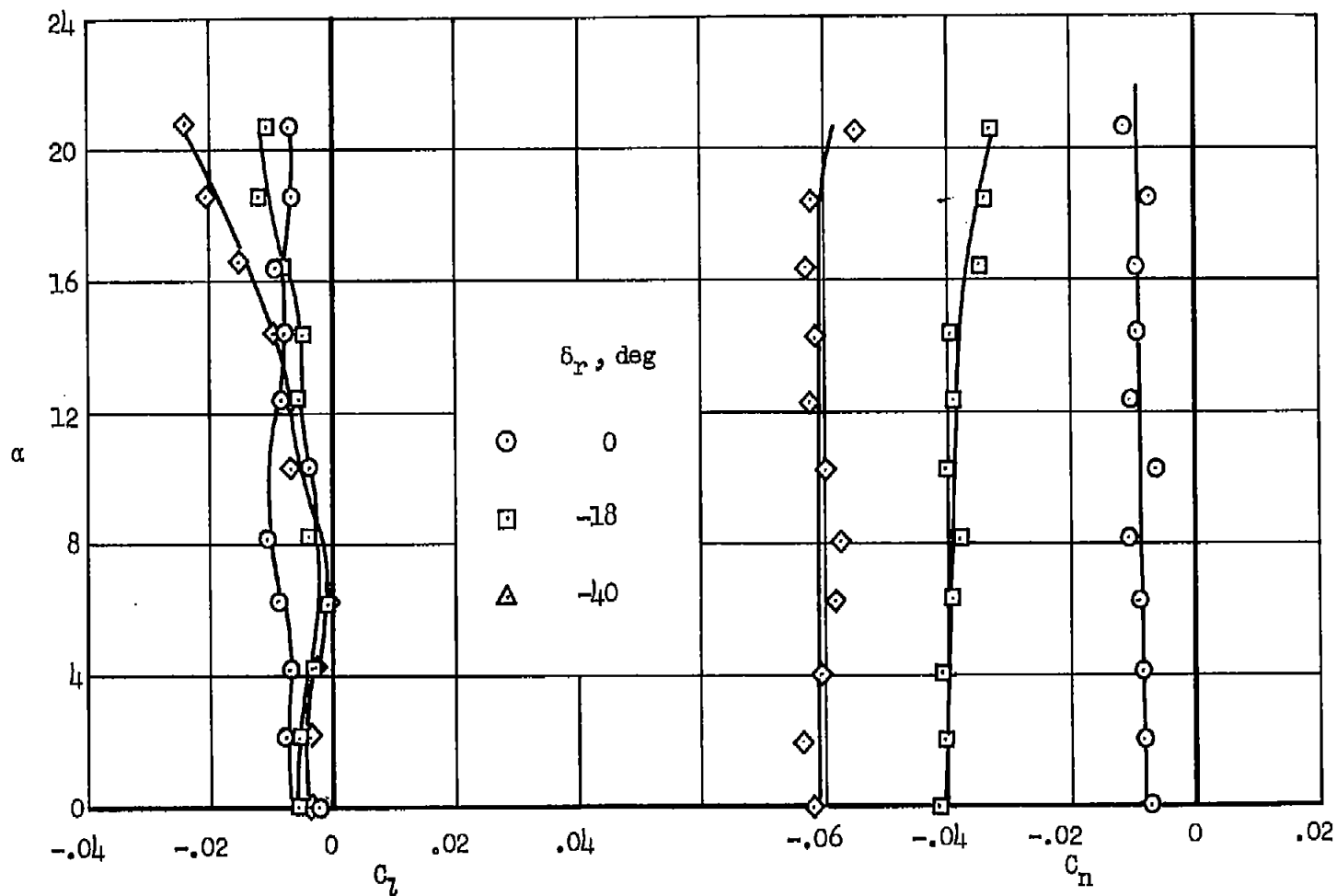


Figure 14.- Variation of C_7 and C_n with α_u and δ_r ; plan form C with twin vertical fins.

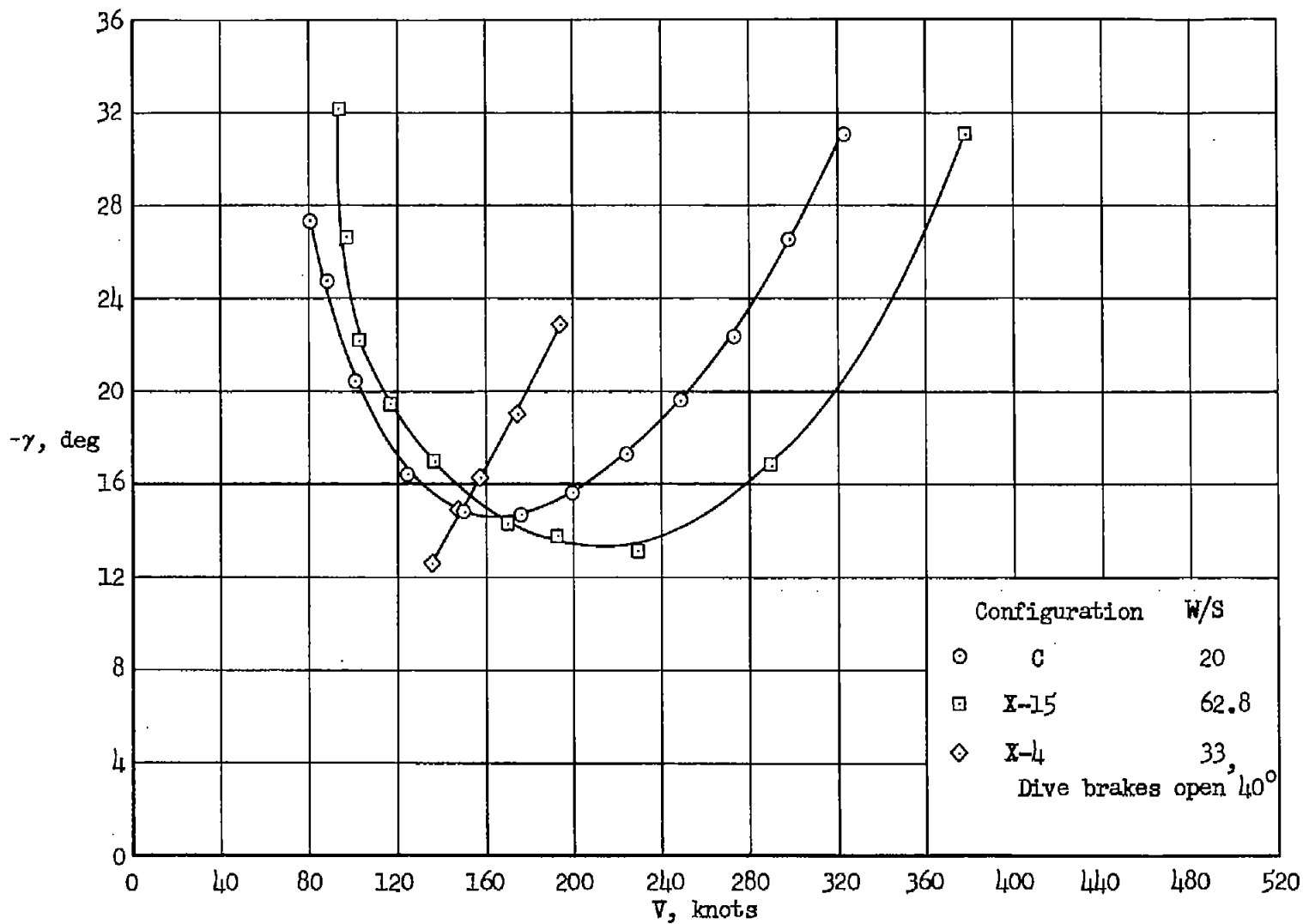


Figure 15.- Variation of power-off glide angle with flight speed for unaccelerated flight.

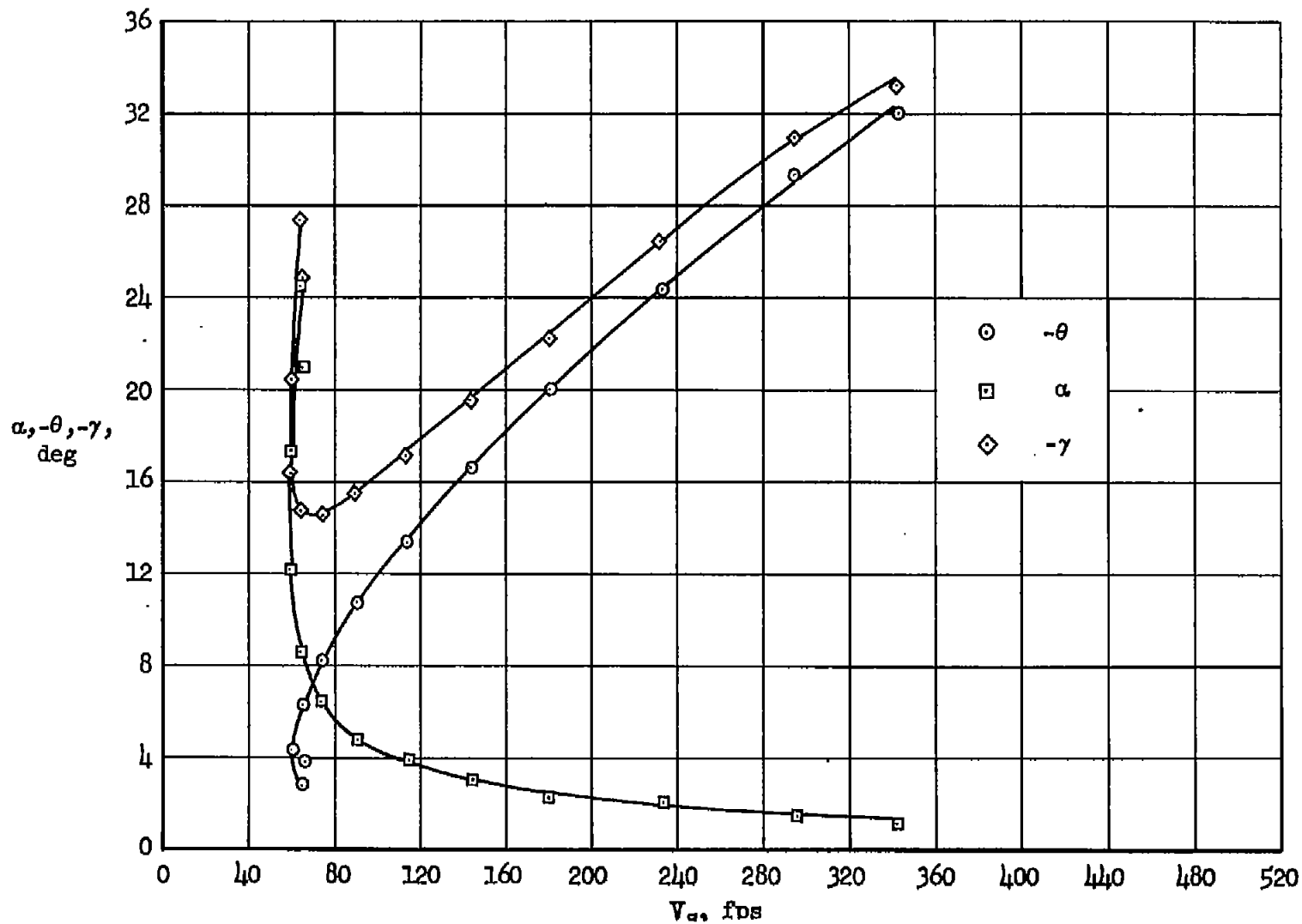


Figure 16.- Variation of angle of attack, glide angle, and attitude angle with sinking speed for unaccelerated flight; plan form C, $W/S = 20$ psf.

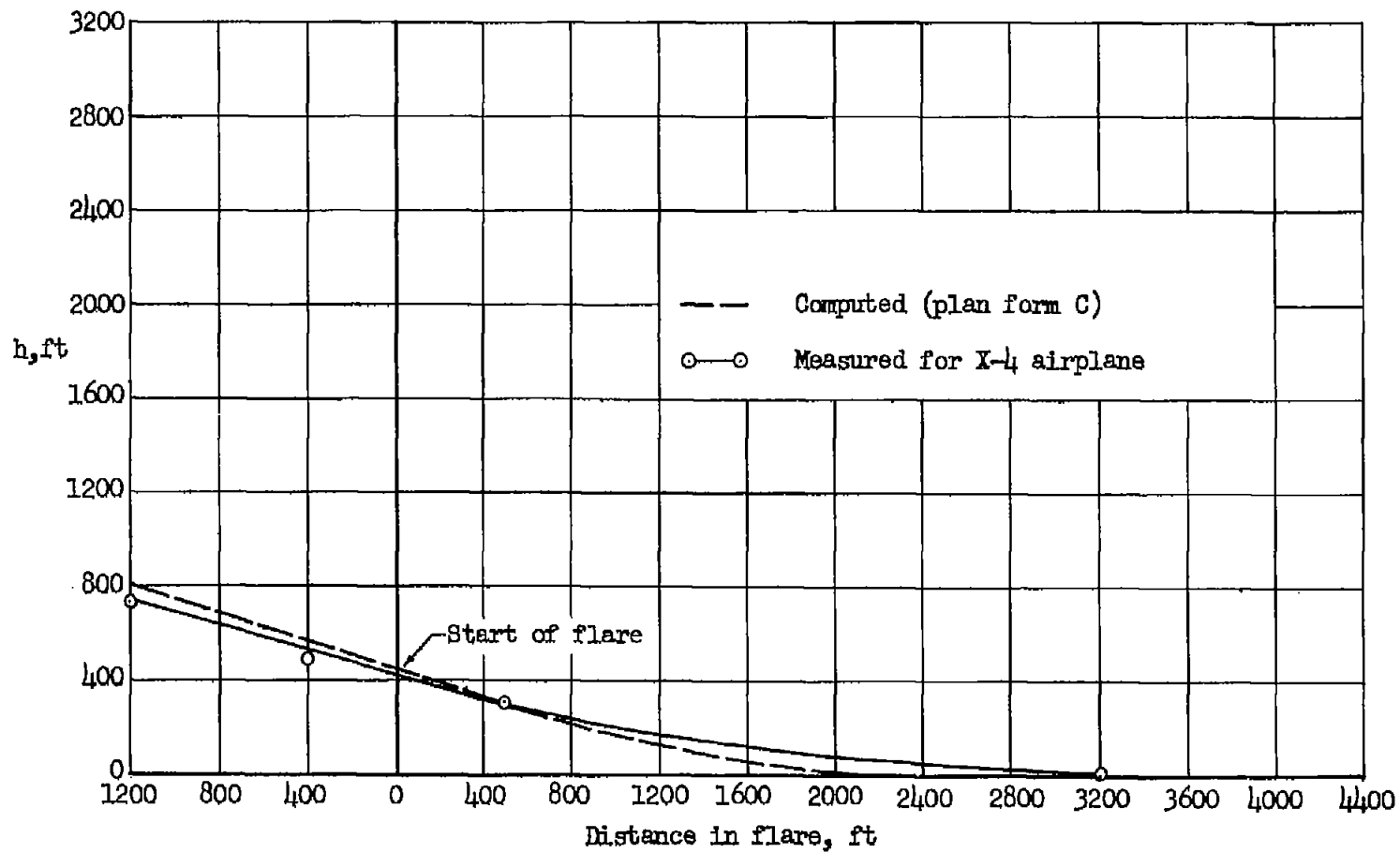


Figure 17.- Comparison of computed landing flare with measured landing flare for the X-4 airplane.

[REDACTED]



LANGLEY RESEARCH CENTER

3 1176 00190 8673



[REDACTED]

[REDACTED]

[REDACTED]